Binbin Zhang
Manufacturing and Design (MAD) Lab,
Department of Mechanical and
Aersopace Engineering,
University at Buffalo (UB)-SUNY,
318 Jarvis Hall,
Buffalo, NY 14260
e-mail: bzhang25@buffalo.edu

Prakhar Jaiswal
Manufacturing and Design (MAD) Lab,
Department of Mechanical and
Aersopace Engineering,
University at Buffalo (UB)-SUNY,
318 Jarvis Hall,
Buffalo, NY 14260
e-mail: prakharj@buffalo.edu

Rahul Rai[1]
Manufacturing and Design (MAD) Lab,
Department of Mechanical and
Aersopace Engineering,
University at Buffalo (UB)-SUNY,
318 Jarvis Hall,
Buffalo, NY 14260
e-mail: rahulrai@buffalo.edu

Saigopal Nelaturi
Palo Alto Research Center,
3333 Coyote Hill Road,
Palo Alto, CA 94304
e-mail: saigopal.nelaturi@parc.com

Additive Manufacturing of Functionally Graded Material Objects: A Review

Functionally graded materials (FGM) have recently attracted a lot of research attention in the wake of the recent prominence of additive manufacturing (AM) technologies. The continuously varying spatial composition profile of two or more materials affords FGM to possess properties of multiple different materials simultaneously. Emerging AM technologies enable manufacturing complex shapes with customized multifunctional material properties in an additive fashion. In this paper, we focus on providing an overview of research at the intersection of AM techniques and FGM objects. We specifically discuss FGM modeling representation schemes and outline a classification system to classify existing FGM representation methods. We also highlight the key aspects such as the part orientation, slicing, and path planning processes that are essential for fabricating FGM object through the use of multimaterial AM techniques. [DOI: 10.1115/1.4039683]

1 Introduction

Functionally graded material (FGM) objects belong to heterogeneous objects that are characterized by gradually varying multiple phase properties (i.e., microstructure and mechanical properties, etc.). Heterogeneous objects refer to objects with different material compositions or structures. Some of the typical examples of heterogeneous objects are objects with FGM distribution, multimaterial objects, embedded sensors/actuators, micro-electro-mechanical systems devices, porous structures, and composites [1,2]. In this paper, we use terms multimaterial and FGM interchangeably for convenience.

Functionally graded material objects have found wide applications in domains such as aerospace [3–6], medicine [3,7–10], energy [11,12], and optoelectronics [13–16]. Aerospace structures require materials to have high specific strength along with high service temperature. The capability of FGM of incorporating several contrasting functions into a single material makes it suitable for use in aerospace structures [17–21]. For example, an FGM made of ceramic and metal provides thermal protection and load carrying capability in one object, thus eliminating the problem of cracked tiles found on the space shuttle [22]. Furthermore, functional gradients are also observed in human organs and tissues. FGMs were fabricated for biomedical application, especially for an artificial bone implant for medical use, artificial tooth implant for dental use [9], and tissue engineering scaffolds [7,23–25]. For example, depending on the necessity of implants, the composition change, from 100% biocompatible metal Ti to fully concentrated ceramic hydroxyapatite (HAp) could control the functions of mechanical properties and biocompatibility. FGM are also developed for energy conversion applications [26–28]. They are not only applied to devices such as turbine blades in gas turbine engines but also devoted as a thermoelectric converter for energy conservation. FGM is also widely used in optoelectronic devices, for example, antireflective layers, fibers, FRIN lens, sensors, and other passive elements made of dielectrics [29–31].

A number of review papers have been published on different aspects of FGM, such as functionally graded composites, the area of applications, and conventional processing techniques [3,32,33]. Nevertheless, the FGM object fabrication through additive manufacturing (AM) technologies has yet to be systematically addressed in any review despite the importance and recent extensive progress in both the topics. The current development in multimaterial AM technology gives us the ability to make complex shapes with customized multifunctional material properties. A key focus of this review is providing an overview of the state-of-the-art multimaterial AM processes.

The multimaterial manufacturing capabilities have far outpaced the modeling capability of design systems to model and thus design novel FGM objects. Limited modeling and lack of suitable representation techniques for modeling and representing FGM objects hinder our ability to leverage the full capabilities of FGM

[1]Corresponding author.

Manuscript received August 20, 2017; final manuscript received March 15, 2018; published online July 3, 2018. Assoc. Editor: Yong Chen.

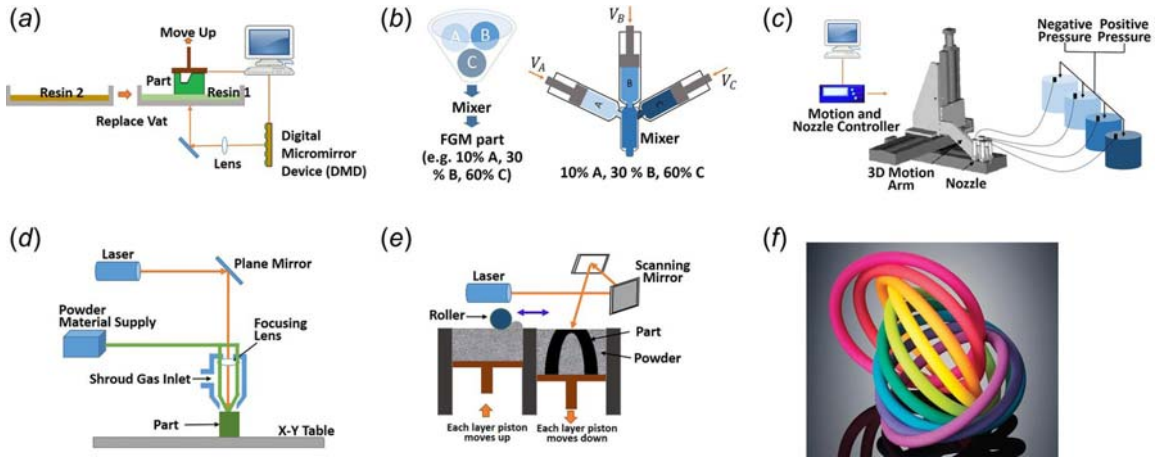

Fig. 1 Manufacturing techniques for FGM objects: (*a*) multimaterial SL process based on bottom-up projection [42], (*b*) triple-extruder mechanism design [44], (*c*) multinozzle deposition for constructing of three-dimensional (3D) scaffolds system setup [45], (*d*) schematic diagram of LENS technique [46], (*e*) schematic diagram of SLM technique [47], and (*f*) 3D printed interlocking color rings with Connex 3 using cyan-magenta-yellow palette [48]

objects creatively. Therefore, the second focus of this review is to provide an overview of modeling and representation of FGM objects. Additionally, additively fabricating a quality FGM object necessitates careful consideration of important aspects such as the part orientation, slicing, and path planning processes. The process planning considerations at the intersection of FGM and AM is the third critical issue that is discussed in this paper.

In this paper, the contents are organized in the following order: In Sec. 2, state-of-the-art multimaterial AM techniques are briefly reviewed. Section 3 of the paper summarizes the FGM object representation and modeling techniques. Three main aspects of process planning of AM based FGM object fabrication, i.e., part orientation, slicing, and path planning, are discussed in Sec. 4. In the last section, the conclusion and future research direction are presented.

2 Manufacturing Techniques for Functionally Graded Material Objects

The wide range of applications enabled by the FGM objects necessitates the development of low cost and high-efficiency manufacturing techniques. There are a variety of manufacturing techniques for fabricating FGM objects. One way to categorize these techniques is based on the type of FGM objects manufactured by them [33]. Mahamood et al. [3] classified the FGM objects into two groups—thin FGM and bulk FGM.

The thin FGM is usually in the form of surface coatings. They are usually produced by vapor deposition techniques (such as sputter deposition, chemical vapor deposition and physical vapor deposition), plasma spraying, and self-propagating high-temperature synthesis (SHS) [3,34]. A major drawback of these methods is the requirement of high energy intensity for depositing thin multimaterial surface coatings. These techniques are also not environmentally friendly [3].

An active area of research and development is the fabrication of bulk FGM. Existing manufacturing techniques for bulk FGM are powder metallurgy, centrifugal method, and AM [3,35,36]. Powder metallurgy has demonstrated the capability of fabricating FGM with varying mechanical properties. However, the property variation has stepped characteristics, whereas a continuous variation in material property is the desired goal. Centrifugal method is capable of creating continuous structures, but this technique has a major limitation of producing objects with radial gradients only. On the other hand, significant aspects of AM techniques are its capability to make geometrically complex objects in a shorter time with less waste. Additionally, the multimaterial AM techniques have recently attracted significant research attention with respect to modeling and fabrication of multifunctional objects [37–40]. In theory, if the composition of the material could be changed from one location to the other during the process to make products with varied composition, the system has the potential of fabricating FGM objects. Some of the AM techniques that could be used to manufacture free-from FGM parts are briefly described below. These techniques differ from each other in terms of the applicable type of *materials and manufacturability restrictions* by the machine [41].

2.1 Vat Photopolymerization Process: Stereolithography. Stereolithography has attractive attributes of creating objects with a high-quality surface finish (e.g., the layer height can achieve between 10 and 100 μm for DWS Lab Xfab® printer), dimensional accuracy, and a variety of material options [42]. The working principle of an SLA process is to solidify each layer of photopolymer liquid resin with an ultraviolet laser. The input material is in liquid form and kept in a vat. The parts are produced in line by line or layer by layer fashion. The material distribution is homogeneous in a layer, but changes along the build direction. It is challenging to attain heterogeneous material compositions within intralayer.

However, there is a possibility of obtaining functionally graded material with SLA. As shown by Zhou et al. [42] and Huang et al. [43], a mask-image-projection-based stereolithography (Fig. 1(*a*)) is proposed to build objects with multiple materials. Mask-image-projection-based stereolithography is realized by utilizing multiple tanks filled with different resins. These tanks are transited in an organized way to change resins. For each layer, the resins within the coverage of projected mask images receive laser rays and solidify. It demonstrated the potential of creating FGM objects with desired mechanical properties, but the efficiency of the process is still a concerning issue.

2.2 Material Extrusion Process: Fused Deposition Modeling. Fused deposition modeling (FDM) produces parts by extruding filaments of molten thermoplastics material through heated nozzles. After extrusion from the nozzle in a desired pattern, the material hardens to form the object. There are large varieties of materials that can be used in FDM process. The

commonly used materials of the filament are acrylonitrile butadiene styrene, polylactic acid, polycarbonate, polyamides, polystyrene, polyethylene, polypropylene. These materials are used due to their high strength and heat resistance properties [49]. FDM devices with multiple nozzles have the potential of additively fabricating functionally graded material objects as long as the machine system allows for an arbitrary mixture of different filament materials. For example, Leu et al. [44] developed a triple-extruder mechanism, which can control the pastes extrusion for desired composition gradients (Fig. 1(*b*)).

Khalil et al. [45] showed the possibility of constructing heterogeneous tissue with FDM process in medical applications. Their system was based on a setup with four different nozzles that could continuously extrude hydrogels or form single droplet hydrogels with picoliter volumes (Fig. 1(*c*)). In particular, the deposition of functional gradient scaffolds is enabled since the material is in gel state rather than a solid filament.

2.3 Laser-Based Process: Laser Engineered Net Shaping, Selective Laser Sintering/Melting). Laser-based processes are promising technologies for fabricating FGM metal parts with excellent strength, accuracy (50–100 μ), and surface roughness ($<10\,\mu$) (Note: the values vary depending upon the machine type, materials, and geometry of the products) [47,50–53]. Both laser engineered net shaping (LENS) and selective laser sintering/melting use powders as construction unit, the former in blown-powder while the latter in a powder-bed technique. Figures 1(*d*) and 1(*e*) show schematic diagram of LENS and SLM processes. By controlling the composition/ratio of different material powders, they have the potential of producing FGM objects. For example, with laser-based process [54], grading copper to specific regions/volumes of H13 tool steel mold could lead to its higher performance in die casting tools. In contrast, LENS is mainly used for iron-, titanium-, and nickel-based alloys. The number of metals used by SLM is greatly more than LENS. Besides, SLM is preferred over SLS for obtaining high-strength products [47]. Other examples of laser-based FGM parts are functionally graded tungsten carbide and tool steel parts [55], alloys (Waspaloy) and ceramic (Zirconia) parts [50,56] by SLM, TiC and Ti composite [57] by LENS, and Nykon-11 and silica nanocomposites [58] by SLS.

2.4 Material Jetting Process: Polyjet Printing. Polyjet 3D printing jet layers of curable liquid photopolymer onto a build tray and the gradient profile is thus continuous. Besides, it offers exceptional detail, surface smoothness, and precision (20–85 μm for features below 50 mm: depends on machine type, build parameters, and geometry of the products) [48]. For example, Connex 3 [48] offers the ability to create objects by jetting material droplets in a predefined pattern from designated microscale inkjet printing nozzles. With a three-base color system, the material droplets have a wide color range option from 20 palettes, each providing 45–72 colors (Fig. 1(*f*)). However, a shortcoming of this process is that the base color material should satisfy specific desired properties. The process requires a specific range of viscosity and curing temperature of the jetted liquid [42]. This limits the type of material that can be used in this process. Besides, Connex 3 uses manual user inputs in a software tool to divide the model into discrete shells and assign materials for each shell.

2.5 Contemporary Processes and Recent Applications. There are several commercially available multimaterial AM machines that can fabricate FGM objects. Additionally, there are several multimaterial AM technologies in development pipeline [3,33,37,43,59]. For instance, the Multifab machine developed by MIT CSAIL [60] provides a machine vision assisted platform for multimaterial 3D printing. The platform supports simultaneous printing of up to ten different materials and achieves a resolution of at least 40 μm by using inkjet print heads. The Foldem technique developed by Perumal and Wigdor [61] allows users to fabricate heterogeneous object via selective ablation of multimaterial sheets. The xPrint system introduced by Wang et al. [62] supports a liquid-based smart material printing platform and has a large range of printable material from synthesized polymers to natural micro-organism-living cells with a printing resolution from 10 μm up to 5 mm (drop size). MIT media lab developed an integrated computational workflow for design and digital AM of multifunctional heterogeneously structured objects. Their proposed workflow enables virtual-to-physical control of constructs in which structural, mechanical, and optical gradients are attained by a seamless design to manufacturing tool with localized control [63]. Das et al. [64] explored an integration of pulsed photonic sintering into multimaterial AM process in order to produce multifunctional components. Their test results indicate that the system holds tremendous promise concerning multifunctional 3D printing.

There have been a number of applications that in particular take advantage of printed heterogeneous FGM objects. For example, nuclear, aerospace, and automobile industries call for high-integrity joints between Ti-alloys and stainless steels, such as Ti-6Al-4V to 304 L stainless steel [65,66]. Reichardt et al. [67] proved the capability of fabricating gradient alloy component transitioning from Ti-alloy to austenitic stainless steel using multi-powder feeder laser metal deposition. Graded polystyrene concrete structures were fabricated and tested by Duballet et al. [68] to provide both sufficient mechanical resistance and thermal isolations. Additively printed FGM objects are also finding new biomedical applications [69]. For instance, the tissue scaffold, which is fabricated through dispensing-based AM technique, provides a supportive environment for cell attachment, proliferation, and differentiation during tissue formation [70–72]. A bitmap printing approach was adopted by Doubrovki et al. [73] to fabricate multimaterial transtibial prosthetic socket targeting patients with amputated lower limbs.

In the area of optoelectronics, Willis et al. [74] have presented the applications of printed custom optical elements for interactive devices. In addition, the co-continuous polymer composite material is fabricated using the Connex500 3D printer and is designed to achieve enhancements in stiffness, strength, and energy dissipation [75]. Disney researchers fabricated actuated deformable characters as replicas of digital characters using AM technologies. The internal material distribution of the printed characters is optimized to exhibit desired deformation behaviors [76]. A functionally graded combustion-powered robot with its body transitioning from rigid core to soft exterior was designed and 3D-printed by Bartlett et al. [77]. In contrast to traditional fabrication techniques, multimaterial printing offers the possibility of cost-effective automation of fabrication process and provides greater flexibility to locally design the composite architecture in three dimensions [78].

In Sec. 3, we discuss existing multimaterial object representation schemes and their specific attributes.

3 Functionally Graded Material Model Representations

In current CAD modeling, the object is modeled as being composed of a single homogeneous material. Modeling of multimaterial and functionally graded material objects is still not supported by current generation CAD systems. A valid representation method for modeling objects with heterogeneous, functionally graded materials has become crucial to leverage the full capabilities of FGM objects creatively. Many techniques have been proposed for data representation and modeling of multimaterial objects. This section aims to review and classify existing FGM object modeling paradigms. Before presenting the review, we discuss several attributes of the representation schemes in the multimaterial modeling.

3.1 Representation Attributes. Important attributes for representing FGM objects should be identified before developing an FGM modeling scheme. The fundamental attributes of FGM object representation are geometry and material. Various other attributes, such as microstructure, tolerances, and operating condition information, could also be included depending on the application.

3.1.1 Geometric Attribute. Multiple representation schemes have been well developed to model geometric attribute as shown in literature [79–81]. The FGM modeling could be an extension of the conventional geometric representations as described in Sec. 3.2.1. Mathematically, the geometric representation of an object is a subset of 3D Euclidean space (E^3). *r*-sets, which are subsets of E^3 that is bounded, closed, regular, and semi-analytic, are widely accepted as mathematical models for solid physical objects. As summarized by Requicha [81] and Kumar et al. [1], the most commonly used representation techniques include: boundary representation, constructive solid geometry (CSG), spatial decomposition, and function representation.

(a) Boundary representation (B-rep) is the most commonly used representation method in CAD software. Boundaries partition the 3D space into three unambiguous regions: the interior, the boundary (or the surface), and the exterior. The object (interior) is represented by its boundary surface patches. There are varieties of structures that are used to represent the boundary surface or surface patches, such as NURBS, splines, and polygonal meshes. The patches or faces are modeled by boundary curves or edges, and the curves are described by vertices. The data structure in mesh-based B-rep is stored as a table filled by vertices' coordinates of the object. Edges are stored by referencing to vertices and adjacent edges. Faces are represented by the loops of edges or vertices [80].
(b) Constructive solid geometry uses simple primitives (such as cylinders, spheres, cones, blocks) to construct complex objects by applying Boolean operations (union, intersection or difference). The binary tree used in CSG represents an object as a Boolean combination of primitive point sets at leaf nodes. Besides Boolean operations, other operations, for example, blending, twisting, bending, and Minkowski operations can also be applied to construct objects [80,82,83].
(c) Spatial decomposition represents a solid model by partitioning the space into 3D regions called cells. The representation scheme is different based on the restrictions imposed on cells. These cells are usually "glued" together to form the whole solid object [82,84]. They can be in the form of axis-aligned cuboidal blocks (voxel), polyhedrons (e.g., tetrahedrons, hexahedrons), or cubes of different sizes (octrees). For example, in voxel representation, the object is represented by recording the coordinates of cuboidal cells in a specific order.
(d) Function representation (F-rep) defines solids as a set of points satisfying a collection of predicates. Predicates are usually conditions on the sign of real-valued functions f(x, y, z) that can be evaluated at any point in the Euclidean space (E3). The form of the function can be defined via any of the following methods: (a) analytically, (b) a function interpolation algorithm, or (c) with tabulated values and a proper evaluation scheme [39].

3.1.2 Material Composition Attribute. In addition to geometric information, representing material information is also an important aspect of FGM modeling. Representing material information for a nonhomogeneous 3D solid is nontrivial. The complexity in representing material arises because material information adds additional dimensions in the overall representation of FGM models. Additionally, the materials could be defined at multiple different scales depending on the application. The distribution of materials in a region can be represented as a mapping from Euclidean 3D space to material space. Each point in material space represents a unique composition of materials. Although, the AM produced FGM objects are rarely solid but are most often optimized lattice or cellular structures. They can still be modeled as solids by including void as one of the primary materials [79]. (a) The material composition representation at a point in 3D space and (b) the material distribution functions to define the variation of material composition over a region in 3D space are detailed below.

(a) Material Composition Definition: In general, an FGM object would consist of at least two different material compositions. Material composition at every point in FGM object can be represented by a unit vector with positive components. For an object with N kinds of primary materials, the material composition at a point X is defined as a vector with N components, i.e., $M_X = [m_1, m_2, \ldots, m_n, \ldots, m_N]$. The value of each component mn is proportional to the volume fraction of material n at the point $X = (x, y, z)$. The summation of all components Σm_n should be 1. In other words, the geometry and material attribute at the point X in the FGM solid object is represented by a vector of the following form: $(x, y, z, [m_1, m_2, \ldots, m_n, \ldots, m_N])$ [82,85,86]. In reality, a dimensionless point in space cannot have multiple materials assigned to it due to the physics at a molecular level. But for computational purposes, defining material composition at a point is a reasonable assumption to estimate material properties of the object at macro-level. To define the distribution of material over a region material distribution functions could be used that maps each point X in 3D space to a material composition vector MX appropriately.
(b) Material Distribution Functions: The material variation across an object can be encapsulated by defining an appropriate material distribution function. The material distribution is defined using vector-valued functions in 3D space. Shin and Dutta [87] has categorized the material composition functions into four different categories—geometry-independent functions (Cartesian, cylindrical, and spherical coordinates), distance-based functions, blending functions, and sweeping functions. Combinations of these functions can also be used to represent material distributions. These functions can be in the form of analytical, segmental, linear, or nonlinear functions [88]. Wu et al. [88] further subdivided the distance-based functions into two classes. The first distance function-based scheme uses reference feature(s) to compute the distance and define material primitives [85]. However, their work was focused on only evaluating three compositions and two materials variations. The second distance field-based scheme was developed to overcome this shortcoming. The second scheme uses fixed reference features and active gradient source-based material evaluation technique. The material vector, in this case, is defined as $M = f(d)(M_e - M_s) + M_s$, where M_s and M_e are the material composition vectors at the start and the end point of reference composition variations.

Bhashyam et al. [86] have compiled a library of material composition functions that specifies the primary material combinations. The compiled library also lists the corresponding intended applications of the given material combinations. These functions are formulated with respect to the local coordinate system. The designers can choose a particular composition function from the database for designing material distribution and for evaluation. More details on various strategies for defining material distribution are presented in Sec. 3.2.

3.1.3 Other Attributes. Among existing efforts on FGM, the majority of research was devoted to modeling objects with continuous compositional functions, where the FGM is characterized with macroscopic volume fractions that follow material distribution functions [89]. Many other material characteristics should be taken into account by a good FGM representation scheme, such as microstructure [90,91]. It is critical because the physical properties of the FGM are significantly affected by its microstructure [92]. Digital representation and quantification of the spatial arrangement of phases, as well as phase connectivity and phase geometry inside random heterogeneous materials, are key ingredients to support object performance estimation [91].

Various statistical descriptors have been developed to characterize microstructure based on the spatial arrangement of heterogeneities [93]. Recent reviews on material microstructure representation are briefly summarized as follows:

Correlation function scheme: McDowell et al. [94] proposed n-point correlation functions to quantitatively characterize microstructures–property relations. The n-point correlation function is defined as the probability associated with finding the same phase of a material microstructure at all vertices of a random n-vertex polyhedron. Many commonly used microstructure metrics, for example, average grain or precipitate size and shape, and the grain boundary character distribution can be reconstructed from two-point correlation functions. A set of weighted statistical volume elements that encompass microstructure subdomain can be identified by the n-point correlation functions. The statistical volume elements are representative of the entire microstructure and should have equivalent material properties with the entire microstructure.

There is more microstructure information contained in high-order correlation functions compared to low-order statistics, for example, minimum higher cycle fatigue lifetime and true fracture ductility. However, high-order correlation functions consume more computation resources since n^2 number of parameters would have to be defined for an n-point correlation function [91,94,95].

Texture synthesis scheme: Liu and Shapiro [91] formulate the material characterization and reconstruction as a Markov random field texture synthesis, which is an image- based texture reproduction technique widely used in computer graphics. With the assumption that the probability of having the material character at a site is a random field that depends only on its neighborhood, the Markov random field texture syntheses process solves the problem in a simpler and local manner rather than globally. Given digitized material microstructure images, the process reconstructs material microstructure images pixel by pixel. Each pixel's value is obtained by searching from a set of pixels with closely matched neighborhoods.

They proved that since the texture synthesis method preserves the joint distribution of random variables of material's microstructure in a neighborhood, the method also preserves reasonable functions of the microstructure in that neighborhood. Besides, the methods are applicable to isotropic, anisotropic, and multiphase materials [91,96].

Supervised learning scheme: The fundamental idea of the supervised learning approach [96] is that the phase of a reconstructed image pixel is modeled as a function of the phases of neighborhood of its surrounding pixels by fitting the given digitized microstructure images (training data) with a supervised learning model. The fitted supervised learning model is taken as a predictive model to represent the conditional distribution of each pixel's phase given its neighbors' phases. The set of conditional distributions provides a computationally efficient means of generating statistically equivalent reconstructed microstructures. The collection tree supervised learning method applied by Bostanabad et al. [96] has proved to be more computationally efficient than other existing methods and applied to a broad range of microstructures.

The aforementioned schemes are alternative ways for material microstructure representation. However, these schemes focus majorly on the microstructural characteristics for material science rather than CAD representation, analysis, and fabrication. There is a lack of robust and effective models that can translate the material science knowledge to CAD domain and integrate them together to develop a comprehensive depiction of FGM object.

Section 3.2 regarding FGM representation approaches mainly focuses on the attributes pertaining to geometry and material composition. We discuss and categorize various representation schemes developed for FGM objects.

3.2 Functionally Graded Material Representation Approaches. To realize the full potential of FGM objects for various applications, a generic and systematic modeling approach for design, analysis, and fabrication of FGM objects needs to be developed. In this review, existing approaches for modeling FGM are presented. At a high level, there are three classes of representation schemes. The first one is the extension of conventional geometric representation schemes. In essence, the classical solid modeling representation approaches are extended from conventional geometric modeling to address FGM representations. The second class includes schemes wherein the material representation is independent of the geometric information of the FGM object. The last class lays down new mathematical models to depict FGM objects. More detailed discussion on all three representation classes is presented in Secs. 3.2.1–3.2.3.

3.2.1 Conventional Geometric Representation Based Functionally Graded Material Modeling. In the conventional geometric representation-based FGM modeling, the classical geometry attribute is utilized as the basis for representing the material attribute. There exist mapping functions for realizing material composition corresponding to the geometric attribute.

Kumar et al. [1] provided a mathematical framework for FGM modeling for a general object with geometry-dependent material definition. In their proposed method, the modeling of an object S takes geometry as the base attribute. Mathematically, the geometric model, G of an object, is an r-set in Euclidean space E^3 and each point in the object corresponds to a unique geometrical point X in E^3. The material attribute is strictly attached to geometry using a mapping function F. The object is modeled as

$$S = \{G, M\}$$
$$F : G(X) \rightarrow M(X)$$

where F denotes the mapping function from geometric space (E^3) to material attribute space (R^N).

The geometry-dependent representation schemes can be further subdivided into a number of categories based on the geometric representation that forms the basis for material or other attributes representation.

(a) B-rep-based Functionally Graded Material representation: Since B-rep can be used to precisely model complex geometry in CAD systems [97], it is also extended to act as a reliable form for representing FGM object. In a B-rep, as described in Sec. 3.1.1, the geometry of an object can be represented in terms of faces, edges, and vertices on the boundary. For geometry-dependent FGM, the material gradient information is associated with the B-rep of object's geometry. The material composition determination includes the material configuration on the boundary and inside the object. For boundary surface patches, their material composition is determined by assigning material directly to patch vertices and using interpolation methods to obtain material on the patch. For any point inside the object, their material condition can be evaluated by a distance-based material distribution function. The distance utilized is the shortest distance from the corresponding point to the boundary of the object. Their mathematical interpretation can be expressed as:

$$S = \{A_p\}, \qquad p = 1, 2, \ldots, P.$$
$$A_p = \{G(V_p), M_P(V_p)\}$$
$$M_I(q) = F(d(q,p))$$

where A_p is one of the surface patches, $G(V_p)$ and $M_P(V_p)$ denote the geometry and material distribution of the surface patch, $M_I(q)$ denotes the material composition inside the object, and q is an inner query point. $M_I(q)$ is determined by the function F, which is in terms of the shortest distance from the query point to boundary patches $d(q, p)$ [98–102].

(b) Constructive Solid Geometry Based Functionally Graded Material representation: Based on CSG geometric representation, Shin and Dutta [87] introduced heterogeneous primitives (hp-set) and heterogeneous modeling operators (hb-set) to create the data structure for representing a heterogeneous object (h-object). This is also applicable for an FGM object. Mathematically, hp-set is a subset $(G, F(G))$ of the product space $T = E^3 \times R^N$, where $G \subset E^3$ is an r-set and $F(G) \subset R^N$ is the image set of the material mapping F. In general, the mapping F is a collection of material composition functions, and each of them maps geometric points to material compositions. The hb-set is constructed as a Boolean composition of two hp-sets. The hb-set is formulated as [87]

(1) Union operation:

$$(G_1, M_1) \cup_m^* (G_2, M_2) = (G_1 \cup^* G_2, M_1 \oplus M_2)$$
$$= (G_1 \cup^* G_2, M_{1\text{and}2} \vee M_{1\text{out}2} \vee M_{2\text{out}1})$$

(2) Intersection operation:

$$(G_1, M_1) \cap_m^* (G_2, M_2) = (G_1 \cap^* G_2, M_1 \oplus M_2)$$
$$= (G_1 \cup^* G_2, M_{1\text{and}2})$$

(3) Difference operation:

$$(G_1, M_1) -_m^* (G_2, M_2) = (G_1 -^* G_2, M_1 \oplus M_2)$$
$$= (G_1 -^* G_2, M_{1\text{out}2})$$

(4) Partition operation:

$$(G_1, M_1) /_m^* (G_2, M_2) = (G_1, M_1 \oplus M_2)$$
$$= (G_1, M_{1\text{and}2} \vee M_{1\text{out}2})$$

where

$$M_{1\text{and}2} = \alpha \cdot M_1(\underline{x}) + (1-\alpha) \cdot M_2(\underline{x})$$
$$\text{for } \underline{x} \in (G_1 \cap^* G_2)$$
$$0 \le \alpha (= const) \le 1$$
$$M_{1\text{out}2} = w_2 \cdot M_1(\underline{x}) + (1-w_2) \cdot \partial M_2(\underline{x}')$$
$$\text{for } \underline{x} \in (G_1 -^* G_2)$$
$$0 \le w_2 = w_2(d_2) \le 1$$
$$M_{2\text{out}1} = w_1 \cdot M_2(\underline{x}) + (1-w_1) \cdot \partial M_1(\underline{x}')$$
$$\text{for } \underline{x} \in (G_2 -^* G_1)$$
$$0 \le w_1 = w_1(d_1) \le 1$$

The material Boolean operator $(M_1 \oplus M_2)$ is determined by the logical disjunction $(\vee)$ of three operators $(M_{1\text{and}2}, M_{1\text{out}2}, M_{2\text{out}1})$, where α is a constant weight factor for the intersection region, w_i is the ith boundary blending function d_i, the distance from the ith boundary, and ∂M_i denotes the material composition at the point $\underline{x}'$ that lies on the ith geometric boundary of the intersection region and is closest to the query point $\underline{x}$, Fig. 2. The h-object is formed as a finite collection of the hp-sets and hb-sets. Figure 3 shows an example of an h-object satisfying these definitions. The primitives (hp-sets) are combined using union operations (hb-sets) to construct the root h-object.

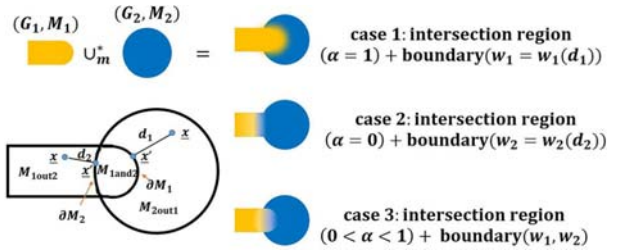

Fig. 2 Three different hb-sets generated by a material union operation [87]

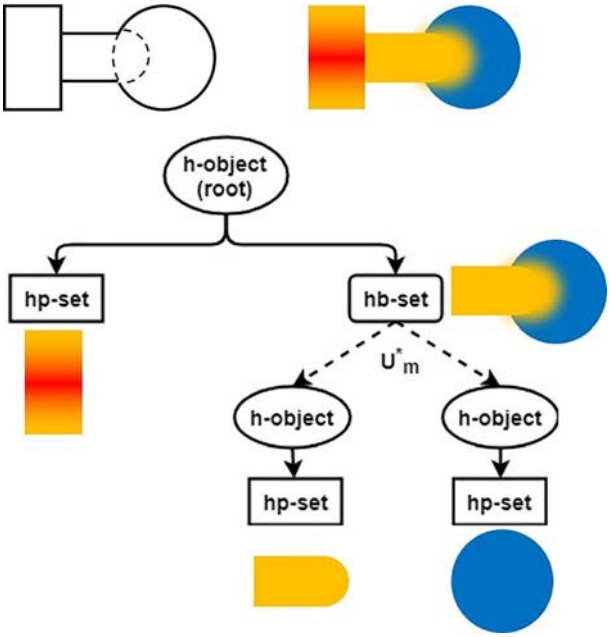

Fig. 3 Model hierarchy in the constructive representation [87]

This representation scheme simplifies the modeling of complex objects from simple primitives in a similar pattern. It is easy and efficient to use for FGM model construction and modification, the memory requirement is low, and the material evaluation queries are accurate. Besides, it can guarantee continuous material composition at interfaces. However, from the intuitiveness point of view, it is not convenient to model FGM objects by defining material distributions on primitives first, and the user's requirements on the objects might not be relevant to these primitives.

(c) Spatial decomposition-based Functionally Graded Material representation: When the geometry of the object is represented with spatial decomposition method, the representation scheme for FGM object is slightly different depending on the form of the decomposed cells. For example, as proposed by Doubrovski et al. [73] and Chandru et al. [103], the FGM object can be decomposed into a set of voxels. Each voxel is defined by its geometric coordinate as well as its material composition. Since the geometric coordinate of each voxel is defined by its center's position, the material

composition of the voxel would be assumed to be the same as its center's material composition. The FGM object is represented as:

$$S = \{V_i\}, \qquad i = 1, 2, \ldots, I.$$
$$V_i = \{(x_i, y_i, z_i, M_i)\}$$

where V_i is the volume element of the FGM object, I is the total number of these volume elements, (x_i, y_i, z_i) is the geometric coordinate of each volume element's center in E^3, and M_i is the corresponding material composition vector of the center. It is important to note that the material composition inside the voxel does not have to be homogeneous. The heterogeneous material data can be obtained through interpolation by using voxel center information [104]. Besides, it is important to choose a suitable resolution of the voxel that approximates both the geometric information and the material composition information with reasonable precision.

Similar to the voxel-based FGM object modeling, mesh-based modeling assigns local material component information to each cell that is in the form of finite element based polyhedrons [98,41,105]. These meshes can also be adaptive as proposed by You et al. [106]. For each polyhedron, the data stored are the coordinates of the polyhedron's vertices and the material compositions at each vertex. The material inside each polyhedron is estimated by an interpolation scheme. Mathematically, the representation model can be expressed as

$$S = \{C_i\}, \quad i = 1, 2, \ldots, I.$$
$$C_i = \{(x_{ij}, y_{ij}, z_{ij}, M_{ij})\}, \quad j = 1, 2, \ldots, J_i.$$
$$M_{ik} = F(x_{ik}, y_{ik}, z_{ik}, C_i), \quad k = 1, 2, \ldots, K$$

where C_i denotes the polyhedron element of the object, I is the total number of polyhedrons, and J_i is the number of vertices for ith polyhedron. $(x_{ij}, y_{ij}, z_{ij}, M_{ij})$ denote the coordinate and material composition of vertices of the ith polyhedron. M_{ik} is the material composition at a point (x_{ik}, y_{ik}, z_{ik}) inside polyhedron C_i that is evaluated using the localized function $F(\cdot)$.

For a general object, the geometric model is appropriately decomposed into several regions for efficient definition and evaluation of material characteristics [1]. Depending on the material attribute M, the geometry G is partitioned into a finite set (with cardinality J) of closed regions U_j. Mathematically

$$S = G \times M = \{(U_j, M_j)\}, \quad j = 1, 2, \ldots, J$$
$$M_j = \{F_j(X \in U_j)\}$$

The material attribute is strictly attached to geometry using a mapping function F. F is a set of functions $F = \{F_j\}$ and each of the F_j maps region U_j in G to material compositions.

In particular, for the case when $J = 1$, it means that there is no spatial partition operated on the object. The geometry and material composition of the object can be interpreted within one region. This is applicable for objects whose material distribution is simple (such as unidirectionally varying material) and can be characterized by a single function. The function can be represented in various forms, such as linear, exponential, parabolic, or power function.

For objects with complex material distributions, J would usually be greater than 1. Several decompositions would be obtained in the geometry model to help in the modeling of material distributions. There are various representation approaches for spatial decompositions, for example, assembly representation and cellular representation [107]. The assembly representation partitions the objects into several parts through direct decomposition or constructive approach. While in cellular decomposition representation, the geometry might be expressed with nonmanifold boundaries due to the material distribution. By introducing the concepts of co-boundaries, the cellular model has better data storage efficiency than the assembly model [107]. For example, Fig. 4(*a*) shows an object with complex material distributions, and Figs. 4(*b*) and 4(*c*) are the assembly representation and cellular model, respectively. The assembly model inheres considerable data redundancy and has low data consistency, for instance, due to the mating faces F_1 and F_2 in Fig. 4(*b*). [82,108]. This phenomenon is alleviated by introducing the co-boundary mechanism [107,109,110]. In this example, the face is uniquely represented with F. F_1 and F_2 are oriented instances of F based on different material compositions. Consistent changes will be applied to both if there are modifications made on the face F.

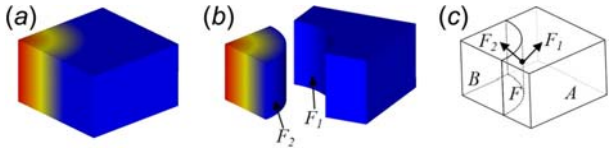

Fig. 4 An example of (*a*) an object with complex material distribution, (*b*) the assembly model of the object, and (*c*) the cellular model of the object [107]

Ability to model very complex FGM objects is the most attractive advantage of spatial decomposition based FGM representation. By adjusting the size and the number of decomposed cells, the accuracy of the representation can be improved. The designer can get the modeled object numerically very close to the actual object by setting the size of the cells small enough, but this comes at the cost of higher computation time and memory space [111]. In addition, the spatial decomposition can be used in conjunction with other material representation techniques, such as B-rep-based FGM representation to get highly concise and accurate representation of FGM models.

(d) F-rep-based Functionally Graded Material representation: In this representation scheme, the geometry of the object is described in the form of functions $f(x, y, z) \geq 0$. The surface/boundary of the object would be the vertices satisfying $f(x, y, z) = 0$, and the interior points are expressed as $f(x, y, z) > 0$ [112]. The material composition is also parameterized in terms of geometric information of the object. The F-rep for the material attribute can be symbolically described as

$$G = \{X = (x, y, z) \in E^3 | f(X) \geq 0\}$$
$$M = \{M_i \in R^N | M_i = F(X)\}$$

where $F : E^3 \rightarrow R^N$ is a material distribution function defined on the 3D Euclidean space [100].

3.2.2 Geometry Independent Functionally Graded Material Object Modeling. When the definition of material is independent of the geometry of an FGM part, it is categorized as geometry-independent material definition. For such objects, the representation schemes for geometry and material can take completely different forms. The geometry can be represented using any of the representation schemes (discussed in Sec. 3.1.1). Similarly, the material distribution can be defined as a vector-valued function in 3D space. The intersection of the geometry in E^3 and the material composition defined as a function $H : E^3 \rightarrow R^N$ results in the

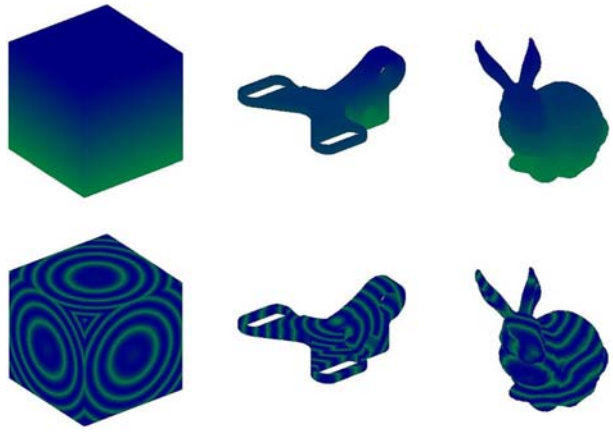

Fig. 5 Examples of Cartesian material definition and objects created using those definitions

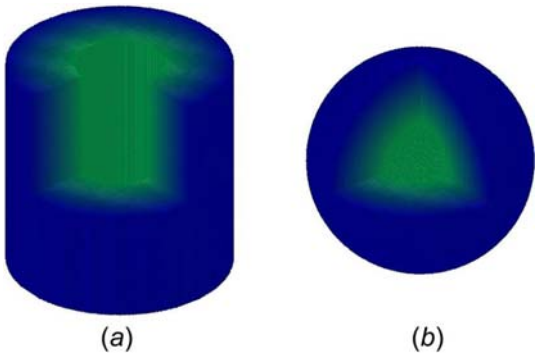

Fig. 6 Partial cross-sectional visualization of material distribution functions defined in (*a*) cylindrical and (*b*) spherical coordinate systems

complete FGM object. This representation scheme simulates the physical process wherein a raw stock is formed by using multiple materials in a certain pattern conforming with the function H and then scooping out the geometrical part using subtractive manufacturing.

There are different categories of functions that could be used for material definition in 3D space, such as linear, nonlinear, discrete, continuous, periodic, and patterned. In addition, these functions can be defined by choosing an appropriate reference coordinate systems (Cartesian, cylindrical, or spherical). The type of coordinate system used enables easier and simpler representation that proves to be useful in various applications and for different geometries of the FGM parts. For example, in case of an axisymmetric model of a pressure vessel, it would be reasonable to use the cylindrical coordinate system.

In a Cartesian coordinate system, the material distribution is defined by an explicit vector-valued function $M = H(x, y, z)$. The material composition can be queried at any point in E^3 within the domain of H irrespective of the geometry of FGM part. A valid material composition function H can be used to define a spectrum of different multimaterial patterns from very simple (such as unidirectionally varying) to highly complex distribution (such as volumetric NURBS-based or local distance-based material distributions). Some examples of material distributions defined in Cartesian coordinate and FGM objects created from those distributions are shown in Fig. 5. Similarly, for applications like axisymmetric parts or ball joints, the cylindrical coordinate or spherical coordinate system would be useful. The material distribution function would be defined as $M = H(r, \theta, z)$ in cylindrical coordinates, or as $M = H(r, \theta, \phi)$ in spherical coordinates. Figure 6 shows examples of material definition in cylindrical and spherical coordinates.

The main advantage of geometry independent material representation scheme is that the material evaluation process is very efficient since the material composition can be directly calculated using the material distribution functions. Furthermore, the independence between geometry and material representations allows for the definition of highly complex geometries as well as highly complex material distributions. One representation does not guide or limit the possibilities available for the other representation.

3.2.3 New Material Primitive-Based Functionally Graded Material Modeling. As discussed in Secs. 3.2.1 and 3.2.2, a number of representation schemes are available for FGM representation. The material information is represented either by extending existing geometric representation or based on the coordinate systems. For conventional geometric representation-based FGM modeling, the material distribution is confined by the geometric structure of the objects. This limits the freedom of modeling irregular and compound material variations. For geometry-independent FGM object modeling, the material configuration has a strong dependence on the coordinate system. From the users' perspective, this may not be favorable in capturing their intentions. Numerous new material primitive-based frameworks have been explored in the literature for a systematic and generic modeling of FGM objects.

The material primitive-based FGM modeling uses simple material primitives, i.e., points, one-dimensional (1D) curves (straight lines or splines), and planes to build complex material distribution. This method is usually preferred from uses' intuitiveness point of view. Multiple algorithms [113–116] have been proposed for material primitive based method. Some of these algorithms are reviewed below.

The *material convolution surfaces-based approach* is presented by Gupta and Tandon [115] for modeling FGM objects with aforementioned material primitives (Fig. 7). The material convolution surfaces are defined as a field function $F(X)$ of material grading enclosure M. The field function $F(X)$ is used to obtain the material composition at an arbitrary point x chosen from a set of points X in space E^3. The material grading enclosure M is a virtual enclosure for modeling simple material distribution, as shown in Fig. 7(*c*). The field function $F(X)$ is defined as the convolution of membership function $b(X)$ and material potential function $f(X)$. The material potential function $f(X)$ is defined by a scheme of material distribution between the extreme positions [117,118] (Fig. 7(*b*))

$$F(X) = b(X) * f(X) = \int_{E^3} b(x) * f(X - x))dx$$

$$b(X) = \begin{cases} 1, & \text{if } X = \{x \in (P \cap M)\} \\ 0, & \text{otherwise} \end{cases}$$

Various material distributions can be efficiently modeled with the material primitives. By adjusting the characteristics of the convolution surface-based material primitives, the material distribution in the object can be improvised correspondingly.

Although the material convolution surface-based scheme is potent for modeling FGM objects, it has the glitches of high data redundancy resulting from unnecessary memory occupation. Besides, it faces the data inconsistency between material and geometry models near boundaries, particularly in the case of spline primitives.

In contrast, Kou and Tan [114] proposed a *hierarchy-based FGM object modeling scheme* by defining different dimensional heterogeneous features. The heterogeneous features are fundamentally material primitives, and they can be in zero-dimensional, one-dimensional, or two-dimensional (2D) features [119]. A heterogeneous feature is characterized by its geometry and material distribution simultaneously. The most fundamental unit in space, a point, is defined first and represented as $P(x, y, z, M)$ in the object representation. The point can be denoted as a zero-dimensional feature. The one-dimensional feature is composed of

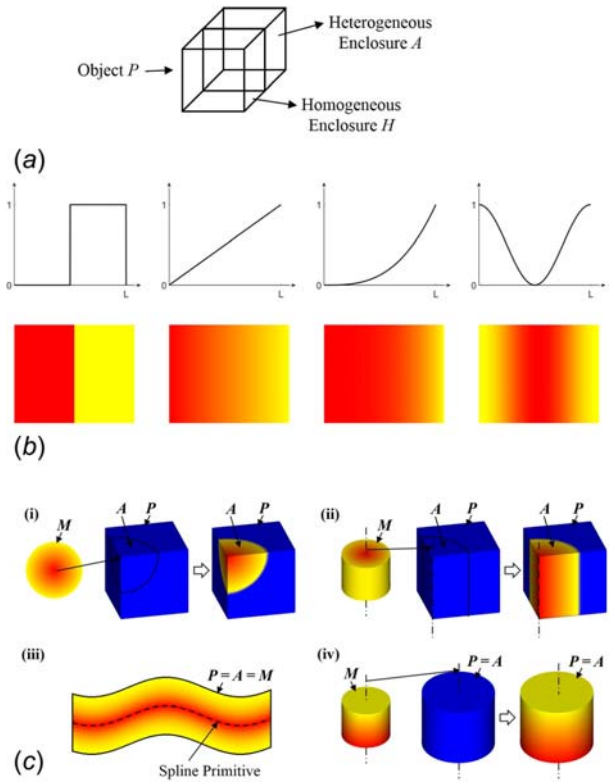

Fig. 7 The material convolution surfaces based approach for FGM modeling [115]: (*a*) Definitions: Object *P*; Heterogeneous enclosure *A*; and Homogeneous enclosure *H*, (*b*) the effect of different material potential functions on material-distribution, (*c*) material modeling with convolution surface-based material primitives (i) Point; (ii) Straight line; (iii) Spline; and (iv) Plane. Note: *M* is Grading enclosure.

a traditional 1D curve and material information that is defined for each point of the 1D curve. For example, as shown in Fig. 8(*a*), a heterogeneous line and B-spline curve with a gradually varying material composition can be described by control points P_i. Mathematically, it can be formulated as

$$P_{(a)} = (1-t)P_s + tP_e, t = \frac{|PP_s|}{|P_sP_e|}, \quad 0 \leqslant t \leqslant 1$$

$$P_{(b)} = \sum_{i=0}^{n-1} w_i P_i$$

where w_i is the blending weight of the ith control point in material gradation. The weight function might be different depending on different types of 1D features [114].

Two-dimensional features are built by combining 1D features. For any point within the 2D region, the material can be defined using 1D features and by applying reverse distance weighing functions w_i as weights [85,104,120,121]. Mathematically, the material in 2D region is defined as

$$M(P) = \sum_{i=0}^{2} w_i M\left(P_{\perp}^{(i)}\right) = \sum_{i=0}^{2} w_i \left(\sum_{j=0}^{1} w_j^{(i)} M\left(P_j^{(i)}\right)\right)$$

$$w_i = \frac{\prod_{j=0, j\neq i}^{2} d_i}{\sum_{k=0}^{2}\prod_{j=0, j\neq i}^{2} d_i}$$

$$d_i = |PP_{\perp}^{(j)}|, \quad j = 0, 1, 2$$

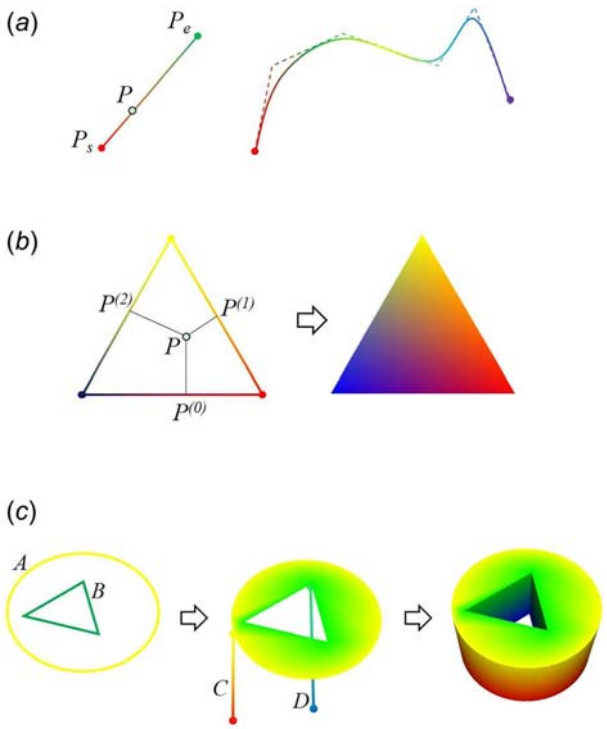

Fig. 8 Hierarchy-based FGM object modeling [114]: (*a*) One-dimensional heterogeneous features, (*b*) two-dimensional heterogeneous features, and (*c*) extruded heterogeneous cylinder

where P is an internal point of the 2D region, $P_{\perp}^{(i)}$ is the orthogonal projection of point P to ith 1D line feature, w_i is the weight of ith line feature, $w_j^{(i)}$ is the weight of jth constructive point on the ith line feature, and $M(\cdot)$ denotes the material composition (Fig. 8(*b*)).

Following similar principle, 3D FGM objects can be extended from 2D features by applying operators like extrusion, revolution, etc. These operators can be a vector, characterized by aforementioned 1D feature.

Based on the hierarchy of features, a heterogeneous feature tree (HFT) is constructed to represent FGM objects. The HFT structure decomposes a 3D solid into a series of lower dimensional entities with specified blending weights. The lower dimensional entities may also be broken down into even lower level nodes. For example, for an extruded heterogeneous cylinder in Fig. 8(*c*), it can be constructed by extruding a 2D region. The 2D region feature is composed of a circle feature A and a triangle feature B. The extrusion of the 2D feature is along two 1D heterogeneous line features C and D. The HFT structure for this model is shown in Fig. 9.

To model complex FGM object with complex geometries efficiently, the extended heterogeneous feature tree (eHFT) [116] has been proposed. eHFT combines the idea of HFT and heterogeneous cellular representation in a single representation framework. An FGM object is decomposed into a set of heterogeneous cells. Each cell resembles separate individual parts [114,119,122]. The eHFT proposes to model the cell-level as well as the overall object-level material distributions. It comprises of an entity-sharing mechanism to reduce data redundancy.

The proposed hierarchical representation is guaranteed to have smooth material transitions throughout the objects and versatile material distributions can be modeled over intricate geometries. On the other hand, material modeling using these material primitives is more perceptive and direct. With properly established material primitives and material distribution functions, the FGM object can be modeled accordingly.

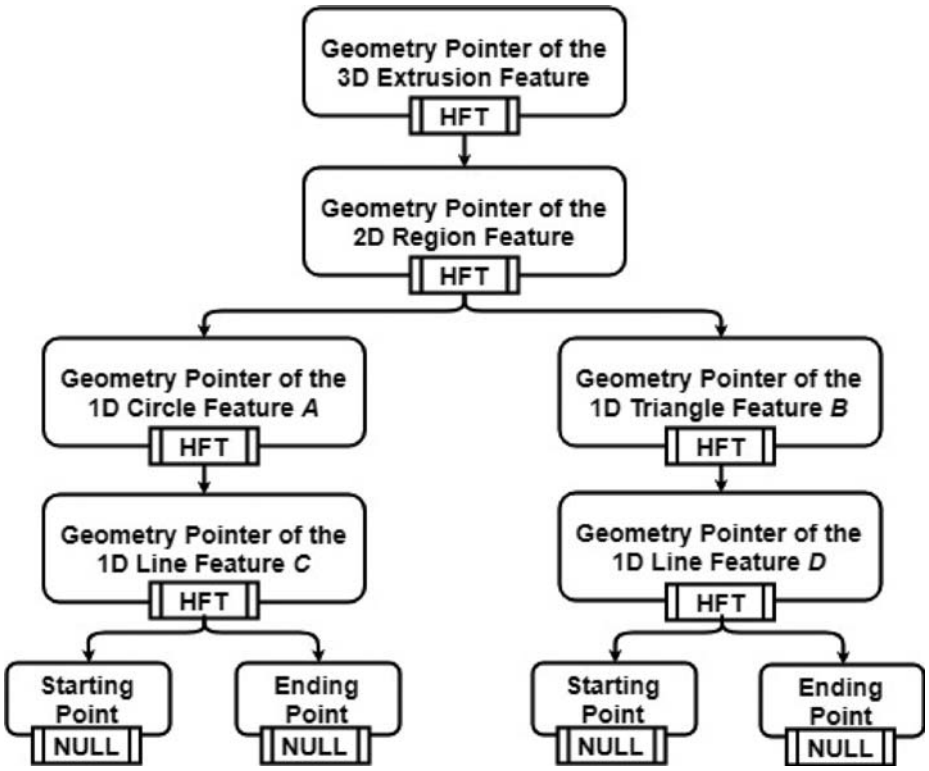

Fig. 9 HFT structure for 3D heterogeneous extrusion solid [114]

3.2.4 What is an Effective Functionally Graded Material Representation Approach?. The variety of FGM representation proposed all have some pros and some cons. It is natural to compare the representations and question, "*Which representation scheme should I use?*" The effectiveness of a representation is usually determined based on its use in downstream applications. In the modern era of computer-aided design (CAD), computer-aided engineering, and computer-aided manufacturing, most tasks in a product's life cycle requires and uses its computer model instead of the physical product. In conventional CAD/ computer-aided engineering / computer-aided manufacturing, often the representations need to be converted from one form to other to support the multitude of operations and computations it is used for. The conversions are required because the representations differ in information content. The systems at different stages of the product lifecycle need various information from the model and work well with representation schemes containing the appropriate information that can be extracted with ease and speed. Representation conversions usually degrade the quality, correctness, and completeness of the information content in addition to being resource consuming [123]. Thus, the choice of representation(s) for an application is driven by the ease, accuracy, and speed with which the required information could be retrieved.

The diversity in the applications of computer representations of a product introduces challenges in forming a single metric to evaluate the effectiveness of representation schemes. There are several key factors, which affect the usability and effectiveness of representation schemes at different stages of the product lifecycle. For instance, during the design phase, the representation should first and foremost support easy and intuitive *creation*. Expert designers and novice users should be able to transform their ideas into computer models using the representation scheme. Other factors such as *level of details*, *flexibility*, *compactness*, and *information retrieval* are also important. The representation scheme should encode features of the models accurately and with sufficient detail. This is necessary for the usability of the model as a substitute to the physical model for computational tasks. It is also necessary for accurate prediction of the performance, realistic simulation, and proper fabrication. Flexibility of representation scheme allows for easy modifications in designs. For industrial components that undergo frequent technological improvements on account of global competition, flexibility of representation is very crucial. Designing a new part with every minor change in design would be highly expensive and time intensive. Thus, minor changes in design should translate to quick changes in a few parameters in the representation of the design. Compactness is another important factor as the storage space is limited and expensive. To exploit the ever-increasing database of 3D designs available online on public repositories, compact representations are necessary. Therefore, the representation should ideally store information in an as low amount of computer memory as possible. Information retrieval is one of the most critical factors for determining the effectiveness of the representation schemes. The type of information sought changes with the application. The information required in a particular application should be easily and quickly retrievable from the representation for it to be deemed suitable for the application.

The information retrieval or queries can be of two types—*evaluation* and *comprehension*. Evaluation is a deterministic and well-defined process wherein the representation contains all the specific information required and can make it explicitly available. On the other hand, in a comprehension process, the information is not present in the representation and must be computed under additional assumptions and imputations [124]. Most applications including performance analysis and manufacturing planning can be formed as a sequence of queries. Hoffmann et al. [125] classified the queries for conventional CAD representations into seven levels numbered from 0 to 6. Studies need to be performed to assess and establish additional queries that would be required for FGM representations involving material gradients. An ideal representation should be able to answer most (if not all) of the queries efficiently with or without the help of computational algorithms.

Table 1 Slicing approaches [126]

Criteria	Technique
Find layer thickness (uniform) from STL file	Marching algorithm Intersect all facets with slicing plane
Find adaptive layer thickness from STL file	Use facet normal information
Find adaptive layer thickness from exact CAD models	Slice at a fixed increment, compare adjacent slices, reslice accordingly Use surface curvature Use wavelet transform Compute exact contours of intersection
	Use existing solid modeler geometry kernel to slice object with a plane Slice primitives, approximate contours with second degree curves, intersect curves to get final part slices Slice NURBS model, approximate contours with bi-arc curves

As shown in Ref. [125], the analysis systems like finite element analysis and computational fluid dynamics can be implemented as a query-based approach. In this approach, the analysis problem is solved by a set of geometric and analysis computations formulated as a sequence of fundamental queries. Similarly, during the manufacturing phase, the optimal orientation identification, slicing, and path planning are tasks that involve querying the model for the required information. To support the manufacturing, an effective representation scheme should allow easy and efficient computations for answering manufacturing queries. Thus, fast and easy retrieval of information is very crucial for an effective representation that is suitable for a multitude of applications.

4 Process Planning for Functionally Graded Material in Additive Manufacturing

Modeling the desired FGM object is followed by a series of processing steps to fabricate the object accurately and efficiently [126]. Although there are a variety of FGM representations and multimaterial AM processes, the process planning steps are similar at the fundamental level. The primary tasks during process planning for AM based FGM object fabrication include part orientation optimization, slicing, and path planning.

4.1 Part Orientation. Part orientation is a critical task in fabrication using AM techniques because it hugely impacts the part accuracy, production time, and manufacturing cost [127]. According to Zhou et al. [37], material features are more important than the part's geometric features when determining the optimal part orientation. With the current techniques of layered manufacturing of FGM objects, it is much easier to print layers with low material variation and high geometric complexity than to print layers with high material variation and low geometric complexity. In an ideal case, the material variation direction would be identical to the printing orientation, i.e., the material composition of each layer would be homogeneous that would be effortlessly printed by the AM machines. Therefore, the part orientation can be determined by minimizing the difference in angles between print orientation and principal material variation direction [37]. However, this is usually only applicable for objects with simplistic material variations.

The part orientation determination problem can be addressed by formulating an optimization model. Zhang et al. [128] developed a perceptual model with a training-and-learning strategy to consider multiple influences of support structures on fabricated objects. The best printing directions are determined by composing all the factors including contact area, visual saliency, viewpoint preference, and smoothness entropy. Cheng et al. [127] formulated a multi-objective function that considers part accuracy and building time as objectives to obtain a suitable build orientation. Various weights are assigned to various surface types affecting part quality to maximize accuracy and minimize building time. Although these algorithms can handle objects with complex surfaces, these implementations are limited to homogeneous object manufacturing. Material features should be incorporated into the objective function formulation for obtaining a suitable part orientation for FGM objects. Although part orientation determination for FGM is affected by a number of other factors [126], the effect of material feature should be furnished special attention.

Hascoët et al. [59] developed a methodology to achieve global control of FGM object part orientation. They classified all typologies of biomaterial gradients using mathematical description. Each typology has an associated accessible part orientation strategy in the manufacturing scheme. Further research is necessary for proposing comprehensive criterion to determine the best strategies for multimaterial parts based on the material, the geometry, and the process parameters considered in conjunction with each other.

4.2 Slicing. Slicing transforms the models into a collection of layers that can then be printed using AM techniques [129]. There are different ways to slice a given solid model. Kulkarni et al. [126] have provided a table summarizing the slicing techniques presented in Table 1.[126] However, the uniform and adaptive slicing algorithms discussed in their paper are only applicable to homogeneous objects, since they do not consider variations in material composition.

Hascoët et al. [59] defined four types of slicing strategies for FGM objects based on the type of deposition surface (planar or complex) and the height of deposition or slices (uniform or non-uniform). The four types of slicing strategies are shown in Fig. 10. They also provide mathematical formulations of these slicing strategies. While decomposing the domain D_m into subdomains $D_{Bj,i}$, it is possible to have a subdomain of entirely homogeneous material, or one-directional gradient, or a 2D gradient of material composition. However, only simple geometric and material distribution was studied by them.

Wu et al. [88], Zhou et al. [37], and Xu and Shaw [130] proposed that the slicing schemes for FGM objects should be determined based on the geometry of the contour and the material distribution in the layer. Wu et al. [88] proposed the

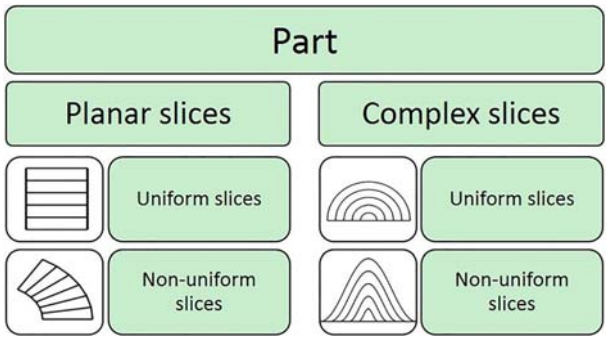

Fig. 10 Representation of classification of types of slices [59]

material resample with geometric constraint for slices of FGM objects. The slicing algorithm essentially comprises of two steps. The first step is to obtain the thickness of geometric slices based on the fabrication demands in the build direction. The second step is sampling each material layer on the geometric contour plane by an interpolation method. This slicing algorithm is based on mesh-based geometric representation. The strategy proposed by Zhou et al. [37] is similar. As the first step, the minimum layer thickness is determined by considering both geometric tolerance and material tolerance. This step is followed by discretizing continuous material distribution into cells/subregions and assessing the material configuration in each cell/subregions. Xu and Shaw [130] utilized the gradient direction of material variation for subregion determination. Then, the detailed material information is inferred based on the FGM representations of material attributes. The shortcoming of these methods is that the retrieval and processing rate of geometric and material information is slow for rapid manufacturing. Moreover, due to sectioning of slices into cells/regions, the fabricated material has low resolution and stair-step effect. Gupta et al. [117] proposed an adaptive slicing technique for AM of heterogeneous objects to reduce errors and minimize the issue of geometry and material stair-step effects.

4.3 Path Planning. The task of path planning involves finding the geometric path and process parameters for each layer/slice of the part locally [126,131]. To quantify the quality of path strategies, Muller et al. [131] proposed the concept of performance indexes. The performance indexes are related to the errors between desired material distributions and real material distribution obtained from the manufacturing process. Path strategies such as raster paths, zig-zag paths, and spiral paths were compared. These basic path strategies can also be utilized for path planning for FGM objects with complex material distribution.

Xu and Shaw [130] studied the path planning for extrusion-based AM process for printing FGM objects. The toolpath of extrusion nozzle was restricted along the iso-composition contours and equal distance offsets (Fig. 11). The iso-composition contour is the contour in each layer that has the same material composition. Additionally, the effect of start and end point selection was also considered in the extrusion process. The criterion for such selection is the minimization of loss of dimensional accuracy due to material over-fill and under-fill.

In manufacturing, there are many other factors that have a significant effect on the mechanical/microstructural property of fabricated objects [132]. For example, Nelaturi and Shapiro [133] accounted for the influence of process limitations and machine imprecision on the accuracy of the as-manufactured model. The as-manufactured model is essentially a substitute for the actual fabricated part. The process uncertainties are due to the variety of factors, such as the printer resolution, uneven material deposition, uncertainty associated with the manufacturing process, imprecision in locating print head while depositing material, etc. Few examples of uncertainty quantification in AM models can be found in papers [134–136]. They have presented techniques to quantify uncertainty in each source, along with algorithms to diminish uncertainty. Bian et al. [137] showed that the performance of fabricated parts is sensitive to several process parameters in direct laser deposition process. These parameters are laser power, traverse speed, powder feed rate, hatch pitch, etc. In addition, the postmanufacturing steps, such as machining and heat treatment, also affect the mechanical/microstructural properties of direct laser deposition parts. In Sec. 5, we conclude the paper by providing a brief summary and discussing some important directions of future work.

5 Conclusion and Open Topics

Additive manufacturing-based FGM object fabrication is one of the most promising areas of research and development. In this paper, we touched upon traditional manufacturing methods and reviewed AM-based processes for FGM object fabrication. Different types of existing FGM object modeling and representation techniques were also discussed. We classify the representation techniques into three classes namely conventional geometric representation-based, geometry-independent, and new material primitive-based FGM representation. The state of the art of process planning pipeline for AM-based FGM object fabrication was also reviewed. Specifically, we discuss different existing methods for part orientation, slicing, and path planning problems. Future research avenues and challenges are discussed next.

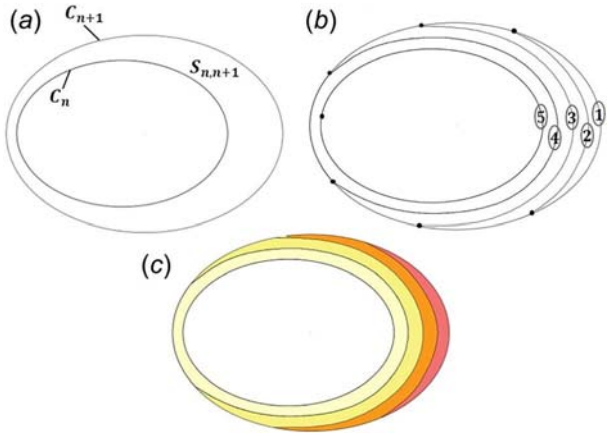

Fig. 11 Process planning of functionally graded objects: (*a*) sub-region $S_{n,n+1}$ between two contours, (*b*) filling toolpaths of the sub-region, and (*c*) the filled region with the rendering effect. The paths 1-5 in (b) represent the filling sequence and (●) stands for the starting and/or ending point for the filling paths [130].

5.1 Functionally Graded Material Modeling and Representation. Modeling of FGM objects is an impeding factor in realizing the full potential of FGM. The limited scope of current CAD tools to handle multimaterial parts hinders our ability to leverage the full capabilities of FGM objects creatively. Some existing FGM modeling paradigms have attempted to represent multimaterial objects. It is crucial that the representation methods are reliable, reasonably accurate, computationally efficient, user-friendly, and easy to modify, share, and store. Existing FGM representation techniques fall short on many of the above-mentioned attributes [138]. A robust representation scheme for FGM objects could be used to develop a conceptual and detailed design tool that assists designers in creating and exploring intricate geometries with complex material distributions. The challenge would be to upgrade current CAD tools to handle varying material composition in a part. Additionally, the tool should be relatively easy to use and intuitive for users to design and define material composition distribution inside the parts. Use of novel human–computer interfaces to create, visualize, and manipulate the 3D model might prove to be convenient and advantageous [139–141]. The FGM representation scheme used in the developed tool should be flexible, accurate, and efficient. Therefore, it is also important to establish criteria to measure the quality and effectiveness of different modeling schemes.

Furthermore, the actual material distribution in a part at a microstructure level would be very difficult to imitate in a virtual model. The variability in interaction behavior of different materials at different operating conditions induces an additional layer of nontriviality in simulating the material structure. For practical purposes, only an approximate model of the material composition that simulates the property of a multi-material part at the macro level with reasonable accuracy and confidence is desired. The model should also be able to account for variability in process

parameters, such as resolutions of material composition in the fabricating system, the temperature variation profile that the material went through during fabrication and any phase changes that occurred and its impact on the material properties at micro and macro levels.

An interesting avenue of future work would be to develop a data-driven approach to complement the creativity and knowledge of designers. For developing a data-driven technique, the primary task would be to create a vast database of material models and its properties. Different combination of materials in different compositions should be tested, and their physical and mechanical properties should be stored in the database. Using suggestive techniques developed in machine learning and probabilistic models for CAD domain [142–144], the database could be used to generate automated suggestions pertaining to the materials to be used for different portions of the designs, the composition of materials to be used, and other topological and geometrical changes to the design.

5.2 Functionally Graded Material Analysis. To simulate the performance of an FGM part, robust and accurate numerical techniques should be developed. The techniques should accurately and efficiently model the performance of any geometrically complex part with complex material distribution under the action of external operating conditions. Several researchers have tried to use classical theories and finite element methods to analyze and model the behavior of FGM objects [132,145,146]. However, these methods could only reason about very simple geometries with unidirectional material variation.

Classical theories of beam, plate, and shell have been adapted to study the different behaviors of FGM parts. The material properties of FGM parts vary in the thickness direction for beams and plates, and in the radial direction for shells according to different laws (such as linear, exponential, and parabolic). The studies involved examining stress, deformation, stability, and vibration of FGM beams (pure FGM beam, sandwich beam with FGM core, and multimaterial beam fused with thin FGM layer), plates (cylindrical, rectangular, circular, and annular), and shells (cylindrical and spherical). It accounted for various effects, such as geometric and physical nonlinearity, and transverse shear deformability. Solution of FGM beams have been obtained using Euler–Bernoulli beam theory, Rayleigh beam theory, Timoshenko beam theory, and first-order shear deformation theory [145,147]. The different behaviors of FGM plates have been studied using the pseudo-Stroh formalism, Stroh complex potential formalism, and first-order and third-order shear deformation theories [148–150]. The analysis of FGM shells including displacement, stress, and thermal behaviors were conducted using the Navier equation, Flugge shell theory, and Donnell shell theory [151,152]. Finite element analysis has also be adapted to simulate the behavior of FGM beams, plates, and shells [145,153,154].

Advanced and robust numerical techniques and a representation scheme that supports analysis computations need to be developed to study and simulate behavior of more complex FGM objects. In addition, it would certainly be beneficial to have a system that can optimize and suggest appropriate changes in the design to satisfy and meet the requirements specified by the designers. The proposed changes could be in the form of change in geometrical parameters of the design, the topology of the design, or the material distribution over critical regions.

5.3 Fabrication and Process Planning for Functionally Graded Material. Compared to traditional manufacturing processes, multimaterial AM systems that enable fabrication of FGM objects require better control on material handling and process parameters. The AM systems have their restrictions on material selection. Besides, the uncertain behavior at the material interfaces has a significant influence on the quality of FGM objects [155,156]. This has hindered the use of AM techniques for fabricating FGM objects. Moreover, some AM techniques are limited to create FGM objects with simple material distributions only (e.g., unidirectional FGM object) [107,119,157–160]. To achieve the desired performance from the FGM object, the process parameters should be properly optimized and controlled to obtain an accurate fabrication. Most current AM systems monitor the process parameters based on operators' experience and trial and error. An extensive study to build a system with highly controllable process parameters to get the desired performance and accuracy is needed. Furthermore, as discussed in Ref. [133], the as-manufactured models are often deviated from the desired objects due to the uncertainty of process parameters and material behavior. A robust design system should incorporate and account for such uncertainties to bridge the gap between the nominal models and the as-manufactured FGM models.

Although representation methods of FGM parts, analysis of its performance in external operating conditions, and its fabrication techniques have been extensively explored, they are rarely comprehensively studied together. An integrated and complete design system that is capable of aiding designer to model, analyze, and fabricate complex FGM objects is yet to be achieved.

References

[1] Kumar, V., Burns, D., Dutta, D., and Hoffmann, C., 1999, "A Framework for Object Modeling," Comput.-Aided Des., **31**(9), pp. 541–556.

[2] Markworth, A., Ramesh, K., and Parks, W., Jr., 1995, "Modelling Studies Applied to Functionally Graded Materials," J. Mater. Sci., **30**(9), pp. 2183–2193.

[3] Mahamood, R. M., Akinlabi, E. T., Shukla, M., and Pityana, S., 2012, "Functionally Graded Material: An Overview," World Congress on Engineering (WCE), London, July 4–6, pp. 1593–1597.

[4] Domack, M., and Baughman, J., 2005, "Development of Nickel-Titanium Graded Composition Components," Rapid Prototyping J., **11**(1), pp. 41–51.

[5] Marin, L., 2005, "Numerical Solution of the Cauchy Problem for Steady-State Heat Transfer in Two-Dimensional Functionally Graded Materials," Int. J. Solids Struct., **42**(15), pp. 4338–4351.

[6] Hirano, T., Teraki, J., and Yamada, T., 1990, "On the Design of Functionally Gradient Materials," First International Symposium on Functionally Gradient Materials, Sendai, Japan, Oct. 8–9, pp. 5–10.

[7] Pompe, W., Worch, H., Epple, M., Friess, W., Gelinsky, M., Greil, P., Hempel, U., Scharnweber, D., and Schulte, K., 2003, "Functionally Graded Materials for Biomedical Applications," Mater. Sci. Eng.: A, **362**(1–2), pp. 40–60.

[8] Matsuo, S., Watari, F., and Ohata, N., 2001, "Fabrication of a Functionally Graded Dental Composite Resin Post and Core by Laser Lithography and Finite Element Analysis of Its Stress Relaxation Effect on Tooth Root," Dent. Mater. J., **20**(4), pp. 257–274.

[9] Watari, F., Yokoyama, A., Omori, M., Hirai, T., Kondo, H., Uo, M., and Kawasaki, T., 2004, "Biocompatibility of Materials and Development to Functionally Graded Implant for Bio-Medical Application," Compos. Sci. Technol., **64**(6), pp. 893–908.

[10] Oonishi, H., Noda, T., Ito, S., Kohda, A., Ishimaru, H., Yamamoto, M., and Tsuji, E., 1994, "Effect of Hydroxyapatite Coating on Bone Growth Into Porous Titanium Alloy Implants Under Loaded Conditions," J. Appl. Biomater., **5**(1), pp. 23–37.

[11] Müller, E., Drašar, Č., Schilz, J., and Kaysser, W., 2003, "Functionally Graded Materials for Sensor and Energy Applications," Mater. Sci. Eng.A, **362**(1–2), pp. 17–39.

[12] Niino, M., Kisara, K., and Mori, M., 2005, "Feasibility Study of FGM Technology in Space Solar Power Systems (SSPS)," Mater. Sci. Forum, **492–493**, pp. 163–170.

[13] Malinina, M., Sammi, T., and Gasik, M. M., 2005, "Corrosion Resistance of Homogeneous and fgm Coatings," Mater. Sci. Forum, **492–493**, pp. 305–310.

[14] Kawasaki, A., and Watanabe, R., 2002, "Thermal Fracture Behavior of Metal/Ceramic Functionally Graded Materials," Eng. Fract. Mech., **69**(14–16), pp. 1713–1728.

[15] Osaka, T., Matsubara, H., Homma, T., Mitamura, S., and Noda, K., 1990, "Microstructural Study of Electroless-Plated Conirep/Nimop Double-Layered Media for Perpendicular Magnetic Recording," Jpn. J. Appl. Phys., **29**(10), p. 1939.

[16] Liu, G., and Tani, J., 1994, "Surface Waves in Functionally Gradient Piezoelectric Plates," ASME J. Vib. Acoust., **116**(4), pp. 440–448.

[17] Librescu, L., Oh, S.-Y., and Song, O., 2005, "Thin-Walled Beams Made of Functionally Graded Materials and Operating in a High Temperature Environment: Vibration and Stability," J. Therm. Stresses, **28**(6–7), pp. 649–712.

[18] Kumar, S., Reddy, K. M., Kumar, A., and Devi, G. R., 2013, "Development and Characterization of Polymer–Ceramic Continuous Fiber Reinforced Functionally Graded Composites for Aerospace Application," Aerosp. Sci. Technol., **26**(1), pp. 185–191.

[19] Richardson, M., 2014, "From Art to Part," Aerospace Manufacturing Magazine, MIT Publishing, Rochester, UK, accessed Feb. 20, 2016, http://www.aero-mag.com/features/63/20141/2265/
[20] Noor, A. K., Venneri, S. L., Paul, D. B., and Hopkins, M. A., 2000, "Structures Technology for Future Aerospace Systems," Comput. Struct., **74**(5), pp. 507–519.
[21] Miyamoto, Y., Kaysser, W., Rabin, B., Kawasaki, A., and Ford, R. G., 2013, *Functionally Graded Materials: Design, Processing and Applications*, Vol. 5, Springer Science & Business Media, New York.
[22] Cooley, W. G., 2005, "Application of Functionally Graded Materials in Aircraft Structures," Air Force Institute of Technology, Wright-Patterson Air Force Base, OH, Technical Report No. AFIT/GAE/ENY/05-M04.
[23] Leong, K., Chua, C., Sudarmadji, N., and Yeong, W., 2008, "Engineering Functionally Graded Tissue Engineering Scaffolds," J. Mech. Behav. Biomed. Mater., **1**(2), pp. 140–152.
[24] Thomas, V., Zhang, X., Catledge, S. A., and Vohra, Y. K., 2007, "Functionally Graded Electrospun Scaffolds With Tunable Mechanical Properties for Vascular Tissue Regeneration," Biomed. Mater., **2**(4), p. 224.
[25] Chua, C., Leong, K., Sudarmadji, N., Liu, M., and Chou, S., 2011, "Selective Laser Sintering of Functionally Graded Tissue Scaffolds," MRS Bull., **36**(12), pp. 1006–1014.
[26] Hazan, E., Ben-Yehuda, O., Madar, N., and Gelbstein, Y., 2015, "Functional Graded Germanium–Lead Chalcogenide-Based Thermoelectric Module for Renewable Energy Applications," Adv. Energy Mater., **5**(11), p. 1500272.
[27] Kambe, M., and Shikata, H., 2002, "Intensive Energy Density Thermoelectric Energy Conversion System by Using FGM Compliant Pads," Acta Astronaut., **51**(1–9), pp. 161–171.
[28] Okano, K., and Takagi, Y., 1996, "Application of Sic-Si Functionally Gradient Material to Thermoelectric Energy Conversion Device," Electr. Eng. Jpn., **117**(6), pp. 9–17.
[29] Wośko, M., Paszkiewicz, B., Piasecki, T., Szyszka, A., Paszkiewicz, R., and Tłaczała, M., 2005, "Applications of Functionally Graded Materials in Optoelectronic Devices," Optica Appl., **35**(3), pp. 663–667.
[30] Wośko, M., Paszkiewicz, B., Piasecki, T., Szyszka, A., Paszkiewicz, R., and Tłaczała, M., 2005, "Application and Modeling of Functionally Graded Materials for Optoelectronic Devices," IEEE International Students and Young Scientists Workshop Photonics and Microsystems, Dresden, Germany, July 7–8, pp. 87–89.
[31] Gupta, K., and Gupta, N., 2015, "Recent Advances and Emerging Trends in Electrical and Electronic Materials," *Advanced Electrical and Electronics Materials: Processes and Applications*, Wiley-Blackwell, Hoboken, NJ, pp. 631–675.
[32] Udupa, G., Rao, S. S., and Gangadharan, K., 2014, "Functionally Graded Composite Materials: An Overview," Procedia Mater. Sci., **5**, pp. 1291–1299.
[33] Kieback, B., Neubrand, A., and Riedel, H., 2003, "Processing Techniques for Functionally Graded Materials," Mater. Sci. Eng.: A, **362**(1–2), pp. 81–106.
[34] Ivosevic, M., Knight, R., Kalidindi, S., Palmese, G., and Sutter, J., 2006, "Solid Particle Erosion Resistance of Thermally Sprayed Functionally Graded Coatings for Polymer Matrix Composites," Surf. Coat. Technol., **200**(16–17), pp. 5145–5151.
[35] Knoppers, G., Gunnink, J., Van Den Hout, J., and Van Vliet, W., 2005, "The Reality of Functionally Graded Material Products," Intelligent Production Machines and Systems-First I* PROMS Virtual Conference, July 4–15, p. 467.
[36] Vidimče, K., Wang, S.-P., Ragan-Kelley, J., and Matusik, W., 2013, "Openfab: A Programmable Pipeline for Multi-Material Fabrication," ACM Trans. Graph. (TOG), **32**(4), p. 136.
[37] Zhou, M., Xi, J., and Yan, J., 2004, "Modeling and Processing of Functionally Graded Materials for Rapid Prototyping," J. Mater. Process. Technol., **146**(3), pp. 396–402.
[38] Zhu, F., 2004, "Visualized CAD Modeling and Layered Manufacturing Modeling for Components Made of a Multiphase Perfect Material," Ph.D. thesis, University of Hong Kong, Hong Kong, China.
[39] Pasko, A., Adzhiev, V., Sourin, A., and Savchenko, V., 1995, "Function Representation in Geometric Modeling: Concepts, Implementation and Applications," Visual Comput., **11**(8), pp. 429–446.
[40] Chiu, W., and Tan, S., 2000, "Multiple Material Objects: From CAD Representation to Data Format for Rapid Prototyping," Comput.-Aided Des., **32**(12), pp. 707–717.
[41] ASTM, 2012, "Standard Terminology for Additive Manufacturing Technologies," ASTM International, West Conshohocken, PA, Standard No. F2792.
[42] Zhou, C., Chen, Y., Yang, Z., and Khoshnevis, B., 2013, "Digital Material Fabrication Using Mask-Image-Projection-Based Stereolithography," Rapid Prototyping J., **19**(3), pp. 153–165.
[43] Huang, P., Deng, D., and Chen, Y., 2013, "Modeling and Fabrication of Heterogeneous Three-Dimensional Objects Based on Additive Manufacturing," ASME Paper No. IMECE2013-65724.
[44] Leu, M. C., Deuser, B. K., Tang, L., Landers, R. G., Hilmas, G. E., and Watts, J. L., 2012, "Freeze-Form Extrusion Fabrication of Functionally Graded Materials," CIRP Ann.-Manuf. Technol., **61**(1), pp. 223–226.
[45] Khalil, S., Nam, J., and Sun, W., 2005, "Multi-Nozzle Deposition for Construction of 3D Biopolymer Tissue Scaffolds," Rapid Prototyping J., **11**(1), pp. 9–17.
[46] Joshi, A., Patnaik, A., Gangil, B., and Kumar, S., 2012, "Laser Assisted Rapid Manufacturing Technique for the Manufacturing of Functionally Graded Materials," Students Conference on Engineering and Systems (SCES), Allahabad, India, Mar. 16–18, pp. 1–3.
[47] Kumar, S., and Pityana, S., 2011, "Laser-Based Additive Manufacturing of Metals," Adv. Mater. Res., **227**, pp. 92–95.
[48] Stratasys, 2018, "Objet500 connex3 white paper," Stratasys, Eden Prairie, MN, accessed Jan. 10, 2016, http://web.stratasys.com/rs/objet/images/SSYS-WP-Objet500 20Connex3.pdf
[49] Boparai, K. S., Boparai, K. S., Singh, R., Singh, R., Singh, H., and Singh, H., 2016, "Development of Rapid Tooling Using Fused Deposition Modeling: A Review," Rapid Prototyping J., **22**(2), pp. 281–299.
[50] Mumtaz, K. A., and Hopkinson, N., 2007, "Laser Melting Functionally Graded Composition of Waspaloy and Zirconia Powders," J. Mater. Sci., **42**(18), pp. 7647–7656.
[51] Fessler, J., Nickel, A., Link, G., Prinz, F., and Fussell, P., 1997, "Functional Gradient Metallic Prototypes Through Shape Deposition Manufacturing," Solid Freeform Fabrication Symposium (SFF), Austin, TX, Aug. 11–13, pp. 521–528.
[52] Muller, P., Mognol, P., and Hascoët, J.-Y., 2013, "Modeling and Control of a Direct Laser Powder Deposition Process for Functionally Graded Materials (FGM) Parts Manufacturing," J. Mater. Process. Technol., **213**(5), pp. 685–692.
[53] Wilson, J. M., and Shin, Y. C., 2012, "Microstructure and Wear Properties of Laser-Deposited Functionally Graded Inconel 690 Reinforced With TIC," Surf. Coat. Technol., **207**, pp. 517–522.
[54] Beal, V., Erasenthiran, P., Hopkinson, N., Dickens, P., and Ahrens, C., 2006, "The Effect of Scanning Strategy on Laser Fusion of Functionally Graded h13/Cu Materials," Int. J. Adv. Manuf. Technol., **30**(9–10), pp. 844–852.
[55] Su, W.-N., 2002, "Layered Fabrication of Tool Steel and Functionally Graded Materials With a ND: Yag Pulsed Laser," Ph.D. thesis, Loughborough University, Loughborough, UK.
[56] Mumtaz, K. A., Erasenthiran, P., and Hopkinson, N., 2008, "High Density Selective Laser Melting of Waspaloy®," J. Mater. Process. Technol., **195**(1–3), pp. 77–87.
[57] Liu, W., and DuPont, J., 2003, "Fabrication of Functionally Graded Tic/Ti Composites by Laser Engineered Net Shaping," Scr. Mater., **48**(9), pp. 1337–1342.
[58] Chung, H., and Das, S., 2008, "Functionally Graded Nylon-11/Silica Nanocomposites Produced by Selective Laser Sintering," Mater. Sci. Eng.: A, **487**(1–2), pp. 251–257.
[59] Hascoët, J., Muller, P., and Mognol, P., 2011, "Manufacturing of Complex Parts With Continuous Functionally Graded Materials (FGM)," Solid Freeform Fabrication Symposium (SFF), Austin, TX, Aug. 8–10, pp. 557–569.
[60] Sitthi-Amorn, P., Ramos, J. E., Wangy, Y., Kwan, J., Lan, J., Wang, W., and Matusik, W., 2015, "Multifab: A Machine Vision Assisted Platform for Multi-Material 3D Printing," ACM Trans. Graph. (TOG), **34**(4), p. 129.
[61] Perumal, C. V., and Wigdor, D., 2016, "Foldem: Heterogeneous Object Fabrication Via Selective Ablation of Multi-Material Sheets," CHI Conference on Human Factors in Computing Systems, San Jose, CA, May 7–12, pp. 5765–5775.
[62] Wang, G., Yao, L., Wang, W., Ou, J., Cheng, C.-Y., and Ishii, H., 2016, "Xprint: A Modularized Liquid Printer for Smart Materials Deposition," CHI Conference on Human Factors in Computing Systems, San Jose, CA, May 7–12, pp. 5743–5752.
[63] Duro-Royo, J., Mogas-Soldevila, L., and Oxman, N., 2015, "Flow-Based Fabrication: An Integrated Computational Workflow for Design and Digital Additive Manufacturing of Multifunctional Heterogeneously Structured Objects," Comput.-Aided Des., **69**, pp. 143–154.
[64] Das, S., Cormier, D., and Williams, S., 2015, "Potential for Multi-Functional Additive Manufacturing Using Pulsed Photonic Sintering," Procedia Manuf., **1**, pp. 366–377.
[65] Dey, H., Ashfaq, M., Bhaduri, A., and Rao, K. P., 2009, "Joining of Titanium to 304l Stainless Steel by Friction Welding," J. Mater. Process. Technol., **209**(18–19), pp. 5862–5870.
[66] Kale, G., Patil, R., and Gawade, P., 1998, "Interdiffusion Studies in Titanium–304 Stainless Steel System," J. Nucl. Mater., **257**(1), pp. 44–50.
[67] Reichardt, A., Dillon, R. P., Borgonia, J. P., Shapiro, A. A., McEnerney, B. W., Momose, T., and Hosemann, P., 2016, "Development and Characterization of Ti-6al-4v to 304l Stainless Steel Gradient Components Fabricated With Laser Deposition Additive Manufacturing," Mater. Des., **104**, pp. 404–413.
[68] Duballet, R., Gosselin, C., and Roux, P., 2015, "Additive Manufacturing and Multi-Objective Optimization of Graded Polystyrene Aggregate Concrete Structures," *Modelling Behaviour*, Springer, Cham, Switzerland, pp. 225–235.
[69] Gupta, A., and Talha, M., 2015, "Recent Development in Modeling and Analysis of Functionally Graded Materials and Structures," Prog. Aerosp. Sci., **79**, pp. 1–14.
[70] Li, M., Tian, X., and Chen, X., 2009, "A Brief Review of Dispensing-Based Rapid Prototyping Techniques in Tissue Scaffold Fabrication: Role of Modeling on Scaffold Properties Prediction," Biofabrication, **1**(3), p. 032001.
[71] Leukers, B., Gülkan, H., Irsen, S. H., Milz, S., Tille, C., Schieker, M., and Seitz, H., 2005, "Hydroxyapatite Scaffolds for Bone Tissue Engineering Made by 3D Printing," J. Mater. Sci.: Mater. Med., **16**(12), pp. 1121–1124.
[72] Cox, S. C., Thornby, J. A., Gibbons, G. J., Williams, M. A., and Mallick, K. K., 2015, "3D Printing of Porous Hydroxyapatite Scaffolds Intended for Use in Bone Tissue Engineering Applications," Mater. Sci. Eng.: C, **47**, pp. 237–247.
[73] Doubrovski, E., Tsai, E., Dikovsky, D., Geraedts, J., Herr, H., and Oxman, N., 2015, "Voxel-Based Fabrication Through Material Property Mapping: A Design Method for Bitmap Printing," Comput.-Aided Des., **60**, pp. 3–13.

[74] Willis, K., Brockmeyer, E., Hudson, S., and Poupyrev, I., 2012, "Printed Optics: 3D Printing of Embedded Optical Elements for Interactive Devices," 25th Annual ACM Symposium on User Interface Software and Technology (UIST), Cambridge, MA, Oct. 7–10, pp. 589–598.
[75] Wang, L., Lau, J., Thomas, E. L., and Boyce, M. C., 2011, "Co-Continuous Composite Materials for Stiffness, Strength, and Energy Dissipation," Adv. Mater., **23**(13), pp. 1524–1529.
[76] Skouras, M., Thomaszewski, B., Coros, S., Bickel, B., and Gross, M., 2013, "Computational Design of Actuated Deformable Characters," ACM Trans. Graph. (TOG), **32**(4), p. 82.
[77] Bartlett, N. W., Tolley, M. T., Overvelde, J. T., Weaver, J. C., Mosadegh, B., Bertoldi, K., Whitesides, G. M., and Wood, R. J., 2015, "A 3D-Printed, Functionally Graded Soft Robot Powered by Combustion," Science, **349**(6244), pp. 161–165.
[78] Studart, A. R., 2016, "Additive Manufacturing of Biologically-Inspired Materials," Chem. Soc. Rev., **45**(2), pp. 359–376.
[79] Kumar, V., and Dutta, D., 1998, "An Approach to Modeling & Representation of Heterogeneous Objects," ASME J. Mech. Des., **120**(4), pp. 659–667.
[80] Rossignac, J. R., and Requicha, A. A., 1999, "Solid Modeling," Georgia Institute of Technology, Atlanta, GA, Technical Report No. GIT-GVU-99-09.
[81] Requicha, A. A., 1980, *Representations of Rigid Solid Objects*, Springer, Berlin.
[82] Kou, X., 2006, "Computer-Aided Design of Heterogeneous Objects," Ph.D. thesis, University of Hong Kong, Hong Kong, China.
[83] Morgan, O., Upreti, K., Subbarayan, G., and Anderson, D., 2015, "Higeom: A Symbolic Framework for a Unified Function Space Representation of Trivariate Solids for Isogeometric Analysis," Comput.-Aided Des., **65**, pp. 34–50.
[84] Shah, J. J., and Mäntylä, M., 1995, *Parametric and Feature-Based CAD/CAM: Concepts, Techniques, and Applications*, Wiley, New York.
[85] Biswas, A., Shapiro, V., and Tsukanov, I., 2004, "Heterogeneous Material Modeling With Distance Fields," Comput. Aided Geometric Des., **21**(3), pp. 215–242.
[86] Bhashyam, S., Hoon Shin, K., and Dutta, D., 2000, "An Integrated CAD System for Design of Heterogeneous Objects," Rapid Prototyping J., **6**(2), pp. 119–135.
[87] Shin, K.-H., and Dutta, D., 2001, "Constructive Representation of Heterogeneous Objects," ASME J. Comput. Inf. Sci. Eng., **1**(3), pp. 205–217.
[88] Wu, X., Liu, W., and Wang, M. Y., 2008, "A CAD Modeling System for Heterogeneous Object," Adv. Eng. Software, **39**(5), pp. 444–453.
[89] Kou, X., and Tan, S., 2012, "Microstructural Modelling of Functionally Graded Materials Using Stochastic Voronoi Diagram and b-Spline Representations," Int. J. Comput. Integr. Manuf., **25**(2), pp. 177–188.
[90] Rosen, D. W., Jeong, N., and Wang, Y., 2013, "A Method for Reverse Engineering of Material Microstructure for Heterogeneous CAD," Comput.-Aided Des., **45**(7), pp. 1068–1078.
[91] Liu, X., and Shapiro, V., 2015, "Random Heterogeneous Materials Via Texture Synthesis," Comput. Mater. Sci., **99**, pp. 177–189.
[92] Latief, F., Biswal, B., Fauzi, U., and Hilfer, R., 2010, "Continuum Reconstruction of the Pore Scale Microstructure for Fontainebleau Sandstone," Phys. A: Stat. Mech. Appl., **389**(8), pp. 1607–1618.
[93] Ghosh, S., and Dimiduk, D. M., 2011, *Computational Methods for Microstructure-Property Relationships*, Springer, New York.
[94] McDowell, D., Ghosh, S., and Kalidindi, S., 2011, "Representation and Computational Structure-Property Relations of Random Media," JOM J. Miner., Met. Mater. Soc., **63**(3), pp. 45–51.
[95] Li, D., 2014, "Review of Structure Representation and Reconstruction on Mesoscale and Microscale," JOM, **66**(3), pp. 444–454.
[96] Bostanabad, R., Bui, A. T., Xie, W., Apley, D. W., and Chen, W., 2016, "Stochastic Microstructure Characterization and Reconstruction Via Supervised Learning," Acta Mater., **103**, pp. 89–102.
[97] Liu, H., 2000, "Algorithms for Design and Interrogation of Functionally Graded Material Solids," Ph.D. thesis, Massachusetts Institute of Technology, Cambridge, MA.
[98] Jackson, T. R., 2000, "Analysis of Functionally Graded Material Object Representation Methods," Ph.D. thesis, Massachusetts Institute of Technology, Cambridge, MA.
[99] Hughes, J. F., van Dam, A., McGuire, M., Sklar, D. F., Foley, J. D., Feiner, S. K., and Akeley, K., 2013, *Computer Graphics: Principles and Practice*, 3rd ed., Pearson Education, Upper saddle river, NJ.
[100] Adzhiev, V., Kartasheva, E., Kunii, T., Pasko, A., and Schmitt, B., 2002, "Cellular-Functional Modeling of Heterogeneous Objects," Seventh ACM Symposium on Solid Modeling and Applications (SMA), Saarbrücken, Germany, June 17–21, pp. 192–203.
[101] Park, S.-M., Crawford, R. H., and Beaman, J. J., 2001, "Volumetric Multi-Texturing for Functionally Gradient Material Representation," Sixth ACM Symposium on Solid Modeling and Applications (SMA), Ann Arbor, MI, June 6–8, pp. 216–224.
[102] Kumar, V., and Dutta, D., 1997, "An Approach to Modeling Multi-Material Objects," Fourth ACM Symposium on Solid Modeling and Applications (SMA), Atlanta, GA, May 14–16, pp. 336–345.
[103] Chandru, V., Manohar, S., and Prakash, C. E., 1995, "Voxel-Based Modeling for Layered Manufacturing," Comput. Graph. Appl., **15**(6), pp. 42–47.
[104] Shin, K.-H., 2002, "Representation and Process Planning for Layered Manufacturing of Heterogeneous Objects," Ph.D. thesis, University of Michigan, Ann Arbor, MI.
[105] Hopkinson, N., Hague, R., and Dickens, P., 2006, *Rapid Manufacturing: An Industrial Revolution for the Digital Age*, Wiley, West Sussex, UK.
[106] You, Y., Kou, X., and Tan, S., 2015, "Adaptive Meshing for Finite Element Analysis of Heterogeneous Materials," Comput.-Aided Des., **62**, pp. 176–189.
[107] Kou, X., and Tan, S., 2007, "Heterogeneous Object Modeling: A Review," Comput.-Aided Des., **39**(4), pp. 284–301.
[108] Kou, X., Tan, S., and Sze, W., 2006, "Modeling Complex Heterogeneous Objects With Non-Manifold Heterogeneous Cells," Comput.-Aided Des., **38**(5), pp. 457–474.
[109] Keen, A. A., 1993, "A Non-Manifold Shape Representation," Ph.D. thesis, Texas A & M University, College Station, TX.
[110] Weiler, K., 1988, "The Radial Edge Structure: A Topological Representation for Non-Manifold Geometric Boundary Modeling," *Geometric Modeling CAD Applications*, Elsevier Science, North Holland, The Netherlands, pp. 3–36.
[111] Wang, C. C., Leung, Y.-S., and Chen, Y., 2010, "Solid Modeling of Polyhedral Objects by Layered Depth-Normal Images on the GPU," Comput.-Aided Des., **42**(6), pp. 535–544.
[112] Pasko, A., Adzhiev, V., Schmitt, B., and Schlick, C., 2001, "Constructive Hypervolume Modeling," Graphical Models, **63**(6), pp. 413–442.
[113] Samanta, K., and Koc, B., 2008, "Feature-Based Material Blending for Heterogeneous Object Modeling," *Heterogeneous Objects Modelling and Applications*, Springer, Berlin, pp. 142–166.
[114] Kou, X., and Tan, S., 2005, "A Hierarchical Representation for Heterogeneous Object Modeling," Comput.-Aided Des., **37**(3), pp. 307–319.
[115] Gupta, V., and Tandon, P., 2015, "Heterogeneous Object Modeling With Material Convolution Surfaces," Comput.-Aided Des., **62**, pp. 236–247.
[116] Kou, X., and Tan, S., 2008, "Heterogeneous Object Design: An Integrated Cax Perspective," *Heterogeneous Objects Modelling and Applications*, Springer, Berlin, pp. 42–59.
[117] Gupta, V., Bajpai, V., and Tandon, P., 2014, "Slice Generation and Data Retrieval Algorithm for Rapid Manufacturing of Heterogeneous Objects," Comput.-Aided Des. Appl., **11**(3), pp. 255–262.
[118] Jin, X., and Tai, C.-L., 2002, "Analytical Methods for Polynomial Weighted Convolution Surfaces With Various Kernels," Comput. Graph., **26**(3), pp. 437–447.
[119] Liu, H., Maekawa, T., Patrikalakis, N., Sachs, E., and Cho, W., 2004, "Methods for Feature-Based Design of Heterogeneous Solids," Comput.-Aided Des., **36**(12), pp. 1141–1159.
[120] Rvachev, V. L., Sheiko, T. I., Shapiro, V., and Tsukanov, I., 2001, "Transfinite Interpolation Over Implicitly Defined Sets," Comput. Aided Geom. Des., **18**(3), pp. 195–220.
[121] Shepard, D., 1968, "A Two-Dimensional Interpolation Function for Irregularly-Spaced Data," 23rd ACM National Conference, New York, Aug. 27–29, pp. 517–524.
[122] Kou, X., and Tan, S., 2009, "Robust and Efficient Algorithms for Rapid Prototyping of Heterogeneous Objects," Rapid Prototyping J., **15**(1), pp. 5–18.
[123] Jaiswal, P., Rai, R., and Nelaturi, S., 2016, "Hysteresis in Interoperability: Workflows Involving Multiple Representations of 3D Models," ASME Paper No. DETC2016-59700.
[124] Hoffmann, C. M., Shapiro, V., and Srinivasan, V., 2011, "Geometric Interoperability for Resilient Manufacturing," Purdue University, West Lafayette, IN, Technical Report No. TR-11-015.
[125] Hoffmann, C., Shapiro, V., and Srinivasan, V., 2014, "Geometric Interoperability Via Queries," Comput.-Aided Des., **46**, pp. 148–159.
[126] Kulkarni, P., Marsan, A., and Dutta, D., 2000, "A Review of Process Planning Techniques in Layered Manufacturing," Rapid Prototyping J., **6**(1), pp. 18–35.
[127] Cheng, W., Fuh, J., Nee, A., Wong, Y., Loh, H., and Miyazawa, T., 1995, "Multi-Objective Optimization of Part-Building Orientation in Stereolithography," Rapid Prototyping J., **1**(4), pp. 12–23.
[128] Zhang, X., Le, X., Panotopoulou, A., Whiting, E., and Wang, C. C., 2015, "Perceptual Models of Preference in 3D Printing Direction," ACM Trans. Graph. (TOG), **34**(6), p. 215.
[129] Shin, K.-H., Natu, H., Dutta, D., and Mazumder, J., 2003, "A Method for the Design and Fabrication of Heterogeneous Objects," Mater. Des., **24**(5), pp. 339–353.
[130] Xu, A., and Shaw, L. L., 2005, "Equal Distance Offset Approach to Representing and Process Planning for Solid Freeform Fabrication of Functionally Graded Materials," Comput.-Aided Des., **37**(12), pp. 1308–1318.
[131] Muller, P., Hascoet, J.-Y., and Mognol, P., 2014, "Toolpaths for Additive Manufacturing of Functionally Graded Materials (FGM) Parts," Rapid Prototyping J., **20**(6), pp. 511–522.
[132] Birman, V., and Byrd, L. W., 2007, "Modeling and Analysis of Functionally Graded Materials and Structures," ASME Appl. Mech. Rev., **60**(5), pp. 195–216.
[133] Nelaturi, S., and Shapiro, V., 2015, "Representation and Analysis of Additively Manufactured Parts," Comput.-Aided Des., **67**(C), pp. 13–23.
[134] Moser, D., Fish, S., Beaman, J., and Murthy, J., 2014, "Multi-Layer Computational Modeling of Selective Laser Sintering Processes," ASME Paper No. IMECE2014-37535.
[135] Ma, L., Fong, J., Lane, B., Moylan, S., Filliben, J., Heckert, A., and Levine, L., 2015, "Using Design of Experiments in Finite Element Modeling to Identify Critical Variables for Laser Powder Bed Fusion," International Solid Freeform Fabrication Symposium (SFF), Austin, TX, Aug. 10–12, pp. 219–228.

[136] Lopez, F., Witherell, P., and Lane, B., 2016, "Identifying Uncertainty in Laser Powder Bed Fusion Additive Manufacturing Models," ASME J. Mech. Des., **138**(11), p. 114502.
[137] Bian, L., Thompson, S. M., and Shamsaei, N., 2015, "Mechanical Properties and Microstructural Features of Direct Laser-Deposited Ti-6al-4v," JOM, **67**(3), pp. 629–638.
[138] Jackson, T. R., Cho, W., Patrikalakis, N. M., and Sachs, E. M., 2002, "Memory Analysis of Solid Model Representations for Heterogeneous Objects," ASME J. Comput. Inf. Sci. Eng., **2**(1), pp. 1–10.
[139] Jaiswal, P., Bajad, A. B., Nanjundaswamy, V. G., Verma, A., and Rai, R., 2013, "Creative Exploration of Scaled Product Family 3D Models Using Gesture Based Conceptual Computer Aided Design (C-CAD) Tool," ASME Paper No. DETC2013-12279.
[140] Nanjundaswamy, V., Kulkarni, A., Chen, Z., Jaiswal, P., Verma, A., and Rai, R., 2013, "Intuitive 3D Computer-Aided Design (CAD) System With Multimodal Interfaces," ASME Paper No. DETC2013-12277.
[141] Shankar, S. S., and Rai, R., 2014, "Human Factors Study on the Usage of BCI Headset for 3D CAD Modeling," Comput.-Aided Des., **54**, pp. 51–55.
[142] Jain, A., Thormählen, T., Ritschel, T., and Seidel, H.-P., 2012, "Material Memex: Automatic Material Suggestions for 3D Objects," ACM Trans. Graph. (TOG), **31**(6), p. 143.
[143] Jaiswal, P., Huang, J., and Rai, R., 2015, "Assembly-Based Conceptual 3D Modeling With Unlabeled Components Using Probabilistic Factor Graph," Comput.-Aided Des., **74**, pp. 45–54.
[144] Zhang, B., and Rai, R., 2014, "Materials Follow Form and Function: Probabilistic Factor Graph Approach for Automatic Material Assignments to 3D Objects," ASME Paper No. DETC2014-34064.
[145] Chakraborty, A., Gopalakrishnan, S., and Reddy, J., 2003, "A New Beam Finite Element for the Analysis of Functionally Graded Materials," Int. J. Mech. Sci., **45**(3), pp. 519–539.
[146] Li, X.-F., 2008, "A Unified Approach for Analyzing Static and Dynamic Behaviors of Functionally Graded Timoshenko and Euler–Bernoulli Beams," J. Sound Vib., **318**(4–5), pp. 1210–1229.
[147] Chakraborty, A., and Gopalakrishnan, S., 2003, "A Spectrally Formulated Finite Element for Wave Propagation Analysis in Functionally Graded Beams," Int. J. Solids Struct., **40**(10), pp. 2421–2448.
[148] Pan, E., 2003, "Exact Solution for Functionally Graded Anisotropic Elastic Composite Laminates," J. Compos. Mater., **37**(21), pp. 1903–1920.
[149] Soldatos, K. P., 2004, "Complex Potential Formalisms for Bending of Inhomogeneous Monoclinic Plates Including Transverse Shear Deformation," J. Mech. Phys. Solids, **52**(2), pp. 341–357.
[150] Vel, S. S., and Batra, R., 2002, "Exact Solution for Thermoelastic Deformations of Functionally Graded Thick Rectangular Plates," AIAA J., **40**(7), pp. 1421–1433.
[151] Jabbari, M., Sohrabpour, S., and Eslami, M., 2002, "Mechanical and Thermal Stresses in a Functionally Graded Hollow Cylinder Due to Radially Symmetric Loads," Int. J. Pressure Vessels Piping, **79**(7), pp. 493–497.
[152] Pelletier, J. L., and Vel, S. S., 2006, "An Exact Solution for the Steady-State Thermoelastic Response of Functionally Graded Orthotropic Cylindrical Shells," Int. J. Solids Struct., **43**(5), pp. 1131–1158.
[153] Della Croce, L., and Venini, P., 2004, "Finite Elements for Functionally Graded Reissner–Mindlin Plates," Comput. Methods Appl. Mech. Eng., **193**(9–11), pp. 705–725.
[154] Bhangale, R. K., Ganesan, N., and Padmanabhan, C., 2006, "Linear Thermoelastic Buckling and Free Vibration Behavior of Functionally Graded Truncated Conical Shells," J. Sound Vib., **292**(1–2), pp. 341–371.
[155] Gao, W., Zhang, Y., Ramanujan, D., Ramani, K., Chen, Y., Williams, C. B., Wang, C. C., Shin, Y. C., Zhang, S., and Zavattieri, P. D., 2015, "The Status, Challenges, and Future of Additive Manufacturing in Engineering," Comput.-Aided Des., **69**, pp. 65–89.
[156] Moore, J. P., and Williams, C. B., 2008, "Fatigue Characterization of 3D Printed Elastomer Material," 19th Annual International Solid Freeform Fabrication Symposium (SFF), Austin, TX, Aug. 4–6, pp. 641–655.
[157] Elishakoff, I., Gentilini, C., and Viola, E., 2005, "Three-Dimensional Analysis of an All-Round Clamped Plate Made of Functionally Graded Materials," Acta Mech., **180**(1–4), pp. 21–36.
[158] Huang, J., Fadel, G. M., Blouin, V. Y., and Grujicic, M., 2002, "Bi-Objective Optimization Design of Functionally Gradient Materials," Mater. Des., **23**(7), pp. 657–666.
[159] Yang, J., Liew, K., Wu, Y., and Kitipornchai, S., 2006, "Thermo-Mechanical Post-Buckling of FGM Cylindrical Panels With Temperature-Dependent Properties," Int. J. Solids Struct., **43**(2), pp. 307–324.
[160] Praveen, G., and Reddy, J., 1998, "Nonlinear Transient Thermoelastic Analysis of Functionally Graded Ceramic-Metal Plates," Int. J. Solids Struct., **35**(33), pp. 4457–4476.